

Exoproteome Heterogeneity among Closely Related *Staphylococcus aureus* t437 Isolates and Possible Implications for Virulence

Xin Zhao,^{†,‡,§} Laura M. Palma Medina,^{†,‡} Tim Stobernack,[†] Corinna Glasner,[†] Anne de Jong,[‡] Putri Utari,[§] Rita Setroikromo,[§] Wim J. Quax,[§] Andreas Otto,^{||} Dörte Becher,^{||} Girbe Buist,[†] and Jan Maarten van Dijl^{*,†}

[†]University of Groningen, University Medical Center Groningen, Department of Medical Microbiology, Hanzeplein 1, P.O. Box 30001, 9700 RB Groningen, The Netherlands

[‡]University of Groningen, Groningen Biomolecular Sciences and Biotechnology Institute, Department of Molecular Genetics, 9747 AG Groningen, The Netherlands

[§]University of Groningen, Groningen Research Institute of Pharmacy, Department of Chemical and Pharmaceutical Biology, A. Deusinglaan 1, 9713 AV Groningen, The Netherlands

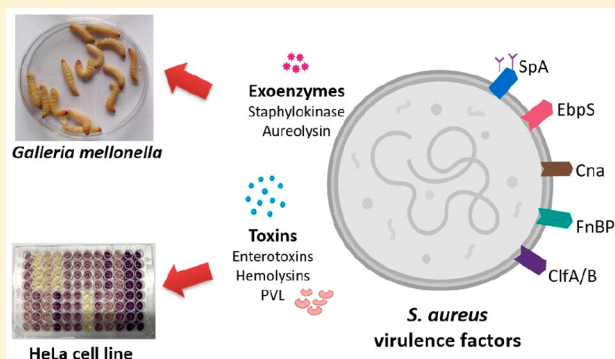
^{||}Institut für Mikrobiologie, University of Greifswald, Felix-Hausdorff-Str. 8, 17475 Greifswald, Germany

Supporting Information

ABSTRACT: *Staphylococcus aureus* with *spa*-type t437 has been identified as a predominant community-associated methicillin-resistant *S. aureus* clone from Asia, which is also encountered in Europe. Molecular typing has previously shown that t437 isolates are highly similar regardless of geographical regions or host environments. The present study was aimed at assessing to what extent this high similarity is actually reflected in the production of secreted virulence factors. We therefore profiled the extracellular proteome, representing the main reservoir of virulence factors, of 20 representative clinical isolates by mass spectrometry. The results show that these isolates can be divided into three groups and nine subgroups based on exoproteome abundance signatures. This implies that

S. aureus t437 isolates show substantial exoproteome heterogeneity. Nonetheless, 30 highly conserved extracellular proteins, of which about 50% have a predicted role in pathogenesis, were dominantly identified. To approximate the virulence of the 20 investigated isolates, we employed infection models based on *Galleria mellonella* and HeLa cells. The results show that the grouping of clinical isolates based on their exoproteome profile can be related to virulence. We consider this outcome important as our approach provides a tool to pinpoint differences in virulence among seemingly highly similar clinical isolates of *S. aureus*.

KEYWORDS: *S. aureus*, ST59, *spa*-type, t437, exoproteome, virulence, *Galleria mellonella*, HeLa cells



INTRODUCTION

The Gram-positive bacterium *Staphylococcus aureus* is a causative agent of different nosocomial and community-acquired diseases that may range from mild superficial skin infections to serious invasive disease.¹ In recent years, *S. aureus* infections have become increasingly difficult to treat due to the acquisition of high-level antibiotic resistance, as underpinned by methicillin-resistant *S. aureus* (MRSA) lineages that are also resistant to other classes of antibiotics.²

To facilitate local surveillance and to monitor the global spread of drug-resistant *S. aureus* lineages, molecular approaches such as multilocus sequence typing (MLST) and *spa*-typing have been developed. These have shown that certain clones of *S. aureus* are frequently prevalent in particular regions of the world. For example, the clone with sequence type (ST) 59, which is linked with the *spa*-type t437, is one of the most dominant community-acquired (CA)-MRSA clones

in Asia³ and Western Australia.^{4,5} In the period from 2016 to 2017, *S. aureus* ST59-MRSA-t437 was reported as the predominant CA-MRSA clone in Chinese children, which appears to relate to a strong ability to form biofilms.⁶ Several studies have shown that the ST59 clone has also spread to European countries.^{7,8} In particular, by MLST and multiple-locus variable number tandem repeat analysis (MLVA) of 147 *S. aureus* isolates with *spa*-type t437 from 11 different European countries, it was shown that these isolates represent a genetically tight cluster irrespective of the country of isolation, the year of isolation or the specific host situation.⁸ It was therefore concluded that the *S. aureus* lineage with *spa*-type t437 has the features of a potentially high-risk clone.

Received: March 14, 2019

Published: May 23, 2019

Table 1. Genotypic and Epidemiological Characteristics of the 20 *S. aureus* t437 Study Isolates

isolate	MLVA complex	MLVA type	country of origin	year of isolation	<i>mecA</i> gene	<i>pvl</i> gene	source
Q1–15	621	1870	France	2004	positive	positive	unknown
Q1–24	621	621	Denmark	2010	positive	positive	SSTI
Q1–54	621	1035	Scotland	2012	positive	positive	skin
Q1–57	621	1297	Spain	2011	positive	negative	SSTI
Q1–59	621	2075	Hungary	2008	positive	positive	throat
Q1–71	621	1875	Netherlands	2005	positive	positive	SSTI
Q1–93	621	621	Netherlands	2006	positive	positive	nose
Q2–101	621	2322	Netherlands	2007	positive	positive	nose
Q2–141	621	4183	Norway	2013	positive	positive	nose
Q2–153	621	621	China	2009	negative	negative	unknown
Q2–146	none	3560	China	2008–2009	positive	positive	unknown
Q2–142	621	621	China	2011	positive	positive	unknown
Q2–116	621	1831	Netherlands	2009	negative	positive	skin
Q3–143	621	621	China	2008–2009	positive	positive	unknown
Q3–147	621	621	China	2010	positive	negative	unknown
Q3–66	621	621	Netherlands	2004	positive	positive	nose
Q3–32	621	4125	Scotland	2008	negative	positive	skin
Q3–107	621	621	Netherlands	2007	positive	positive	wound
Q3–104	621	621	Netherlands	2007	positive	positive	nose

The ability of *S. aureus* to cause infections relates to the expression of a wide variety of virulence factors.⁹ These proteins play decisive roles in promoting the colonization of the human host, invasion of cells and tissues, and evasion of the innate and adaptive immune responses. Interestingly, only few staphylococcal virulence factors, such as the toxic shock syndrome toxin or exfoliative toxins, can be directly associated with particular disease phenotypes.^{10–12} Instead, in most infections a highly potent cocktail of virulence factors is employed by *S. aureus* to breach the barriers imposed by the skin and mucosal tissues and to invade the human body.^{13,14} Early proteomics studies have shown that the assembly of virulence factors produced by *S. aureus* is highly variable for different clonal lineages.¹⁵ This can be attributed in particular to the high genomic plasticity of the *S. aureus* genome, which is shaped by successive events of horizontal gene transfer as exemplified by the presence of prophages, staphylococcal pathogenicity islands, and the staphylococcal cassette chromosome responsible for methicillin resistance. On the other hand, very little is known about possible variations in the production of virulence factors by different clinical isolates of one particular clonal lineage of *S. aureus*. Yet, insights in such variations are needed to understand the extent to which they determine different degrees of staphylococcal virulence and to assess the health risks imposed by individual clinical isolates.

The extracellular proteome (in short exoproteome) of bacterial pathogens, like *S. aureus*, is considered as the main reservoir of virulence factors.^{9,16} In the present study, we profiled the composition of the exoproteomes of 20 clinical *S. aureus* isolates with *spa*-type t437 to assess the extent to which the production of virulence factors and other secreted proteins may vary among this genetically highly homogeneous group of *S. aureus* isolates. As a first approach to assess the possible implications of the observed variations, we employed larvae of the greater wax moth *Galleria mellonella*, an infection model that was previously shown to be susceptible to a range of human pathogens.¹⁷ Importantly, upon injection into the larvae, bacteria are challenged directly by an innate immune system, which is functionally and structurally equivalent to that of mammals.¹⁸ Subsequently, we applied the human HeLa

cancer cell line for high-throughput profiling of invasion and cytotoxicity of the investigated *S. aureus* t437 isolates in nonprofessional phagocytic cells. Briefly, the results of our present study show that the investigated *S. aureus* t437 clinical isolates can be divided into three groups and nine subgroups based on their exoproteome profiles, and that isolates belonging to particular subgroups show similarities in virulence when confronted with the innate immune defenses of *G. mellonella*. In contrast, relatively smaller variations were observed in the HeLa cell infection model, which assays the efficiency of nonprofessional phagocyte invasion and subsequent killing. It thus seems that the observed variations in the exoproteomes of different *S. aureus* t437 isolates do not have the same impact in the two infection models which, most likely, reflects the fact that these models impose different challenges on infecting bacteria. A comparative analysis of the present scale, relating staphylococcal exoproteome composition to virulence, is unprecedented. Importantly, this approach represents an effective pipeline to define proteomic signatures of *S. aureus* virulence.

■ MATERIALS AND METHODS

Bacterial Isolates

A total of 20 *S. aureus spa*-type t437 isolates was used for exoproteome analyses in the present study (Table 1). Ten of these isolates were selected from the MLVA type (MT) 621 group, which has been shown to represent the most predominant class of *S. aureus* t437 isolates; the other ten isolates belong to different MTs as indicated in Table 1.

Bacterial Cultivation and Collection of Extracellular Proteins

Bacterial cultivation and extracellular protein extraction were carried out as described previously.¹⁹ Briefly, all bacterial isolates were grown in triplicate overnight (14–16 h) in 10 mL tryptic soy broth (TSB, OXOID, Basingstoke, UK) under vigorous shaking (115 rpm) at 37 °C in a water bath. The cultures were then diluted into 10 mL prewarmed Roswell Park Memorial Institute 1640 (RPMI) medium supplemented with 2 mM glutamine (GE Healthcare/PAA, Little Chalfont,

United Kingdom) to an optical density at 600 nm (OD_{600}) of 0.1 and cultivation was continued under the same conditions. Exponentially growing cells with an OD_{600} of ± 0.5 were again diluted into 20 mL of fresh prewarmed RPMI 1640 medium to a final OD_{600} of 0.1 and their cultivation was continued until an OD_{600} of ± 1.3 was reached, which corresponds to the stationary growth phase. Then, growth medium fractions were collected by centrifugation. Proteins in the growth medium were precipitated overnight with 10% trichloroacetic acid (TCA, Sigma-Aldrich, St. Louis, USA) on ice. The precipitated proteins were collected by centrifugation. Pellets of precipitated proteins were washed once with ice-cold acetone, dried at room temperature and stored at -20°C until further use.

LDS-PAGE and Western Blotting

To inspect extracellular proteins by lithium dodecyl sulfate (LDS) polyacrylamide gel electrophoresis (PAGE), TCA-precipitated proteins were resuspended in LDS sample buffer and separated on NuPAGE gels (Life Technologies, Grand Island, NY, USA). The separated proteins were visualized by Simply Blue Safe Staining (Life Technologies). The presence of IsaA was assessed by Western blotting using Protran nitrocellulose transfer paper (Whatman, Germany) and immunodetection using the IRDye 800CW-labeled 1D9 monoclonal antibody that is specific for IsaA.²⁰ Antibody binding was detected using an Odyssey Infrared Imaging System (LI-COR Biosciences, Lincoln, NE, USA).

Protease Activity Profiling

To assess the activity of proteases in the growth medium of the investigated *S. aureus* t437 isolates in the stationary growth phase, we applied His₆-tagged derivatives of the *S. aureus* IsaA and SCIN proteins that were recombinantly produced in *Lactococcus lactis* NZ9700 as described previously.²¹ Specifically, 500 μL aliquots of *L. lactis* growth medium containing recombinant IsaA or SCIN were mixed with 500 μL aliquots of spent growth media (RPMI 1640) of the 20 investigated *S. aureus* t437 isolates and incubated overnight at 37°C . Of note, prior to this incubation, cells of *L. lactis* and *S. aureus* had been removed from the respective growth medium fractions by centrifugation. After the overnight incubation, proteins in the incubation mixtures were precipitated overnight at 4°C with 10% TCA, and separated by LDS-PAGE. The presence of His₆-tagged IsaA or SCIN was then assessed by Western blotting using His₆-specific antibodies (Invitrogen, Canada).

Sample Preparation for Mass Spectrometry

Collected extracellular proteins were processed for Mass Spectrometry (MS) analysis essentially as described previously.²² In brief, the dried protein pellets were resuspended in 50 mM ammonium bicarbonate buffer (Fluka, Buchs, Switzerland) and reduced with 500 mM dithiothreitol (DTT, Duchefa Biochemie, The Netherlands) for 45 min at 60°C . The samples were then alkylated with 500 mM iodoacetamide (IAA, Sigma-Aldrich) and incubated for 15 min in the dark at room temperature. 100 ng of sequencing grade modified trypsin (Promega, Madison, USA) were added and the mixture was incubated overnight at 37°C under continuous shaking at 250 rpm to completely digest the proteins. Subsequently, the samples were acidified with a final concentration of 0.1% trifluoroacetic acid (TFA, Sigma-Aldrich, St. Louis, USA) for 45 min at 37°C to inactivate the trypsin. The digested peptides were purified with C-18 ZipTips (Millipore, Billerica,

USA). The ZipTips were first wetted with 45 μL 70% acetonitrile (ACN, Fluka, Buchs, Switzerland) and then equilibrated with 45 μL 3% ACN/0.1% acetic acid. Peptides were bound to the ZipTips by pipetting 10 times up and down. After washing with 45 μL 0.1% MS-acetic acid, the ZipTips were eluted with 45 μL 60% ACN/0.1% MS-acetic acid. Lastly, the eluted peptides were dried in a SpeedVac (Eppendorf, Hamburg, Germany) at room temperature. The dried samples were stored at 4°C until further use.

Mass Spectrometry Analyses

Purified peptides were identified by reversed-phase liquid chromatography coupled to electrospray ionization mass spectrometry (MS) using an LTQ Orbitrap XL (Thermo Fisher Scientific, Waltham, MA) as described by Stobernack et al.²² In brief, Sorcerer-SEQUENT 4 (Sage-N Research, Milpitas, USA) was applied for database searching, and raw data files were searched with SEQUEST against a target-decoy database. The nonredundant database that was used for protein identifications was based on published genome sequences of the *S. aureus* isolates with ST2147, ST59, or ST338 (downloaded from <https://www.ncbi.nlm.nih.gov/>), which represent the dominant STs of *S. aureus* t437.⁸ This database includes 7187 protein sequences with connected gene names and Uniprot identifiers. Validation of MS/MS-based peptide and protein identification was performed with Scaffold V4.7.5 (Proteome Software, Portland, USA), and peptide identifications were accepted if they exceeded the specific database search engine thresholds. SEQUEST identifications required at least deltaCn scores of greater than 0.1 and XCorr scores of greater than 2.2, 3.3, and 3.75 for doubly, triply and all higher charged peptides, respectively. Protein identifications were accepted if at least 2 identified peptides were detected with the above-mentioned filter criteria in 2 out of 3 biological replicates. Protein data was exported from Scaffold and curated in Microsoft Excel before further analyses (Tables S1 and S2). Since we observed large differences in the total spectral counts, the normalization of the data was not performed over all data sets simultaneously, because this would over-represent the quantities of proteins in samples with fewer protein identifications. Instead, the data sets for different isolates were clustered into three groups (Q1–3) based on the total spectral counts, and each group was mean-normalized as recommended in the Scaffold software for spectral counting data sets (<https://proteomesoftware.zendesk.com/hc/en-us/articles/115002739586-Spectrum-Count-Normalization-in-Scaffold>).

Assessment of Virulence with a *Galleria mellonella* Infection Model

To evaluate the virulence of investigated *S. aureus* t437 isolates using *G. mellonella*, larvae of ~ 250 mg in the final instar stage were purchased (Frits Kuiper, Groningen, Netherlands) and stored in the dark at room temperature. The larvae were used for infection experiments within 7 days of receipt. Until then, they were fed with wood shavings. Prior to an infection experiment, bacteria were grown overnight in TSB medium and collected by centrifugation at $2700g$ for 10 min at 4°C . The cell pellets were washed by resuspension in phosphate-buffered saline (PBS), collected by centrifugation, resuspended in PBS, and diluted to the desired number of colony-forming units (CFU) per mL as approximated based on the optical density at OD_{600} of the overnight culture. Infections were performed by inoculating the larvae with 10 μL aliquots of a

bacterial suspension in PBS (2.5×10^6 CFU) into the hemocoel via the last left proleg using an insulin pen (HumaPen LUXURA HD, Indianapolis, USA).²³ After injection, the larvae were kept in Petri dishes in the dark at 37 °C, and mortality was monitored after 24 and 48 h post infection. Larvae were considered dead when they displayed no movement after being touched with a sterile inoculation loop. The virulence of each investigated *S. aureus* t437 isolate was tested in triplicate using 15 larvae per experiment ($n = 45$), and for each of these three biological replicates larvae from different batches were used. Data from all infection experiments were combined to calculate the average mortality. For control, one group ($n = 15$) of larvae was injected with 10 μ L of PBS to monitor the impact of physical trauma, a second group ($n = 15$) was injected with 2.5×10^7 CFU of heat-killed bacteria to monitor potentially lethal effects caused by toxic bacterial components, and a third group ($n = 15$) received no injection at all.

To verify possible roles in virulence of the extracellularly identified proteins IsdA, IsdB and IsaA, specific single mutant strains and the respective parental strains USA300 LAC (for *isaA* or *isdB* mutations)²⁴ and SH1000 (for the *isaA* mutation)²⁵ were used to infect *G. mellonella* larvae. In this case, the larvae were inoculated as described above, but with 1×10^6 CFU of bacteria. The larval survival was monitored from 24 h until 96 h post infection. Each bacterial isolate was used to inoculate 10 larvae per experiment, and all experiments were performed in triplicate.

Assessment of Staphylococcal Cytotoxicity with a HeLa Cell Infection Model

The human cervical cancer HeLa cell line was cultured in DMEM-GlutaMAX medium (Gibco, UK) supplemented with 10% fetal calf serum (Sigma-Aldrich, USA) at 37 °C and 5% CO₂. 0.25% Trypsin-EDTA (Gibco, UK) was used to detach adherent cells for subculturing. 3×10^4 HeLa cells in a total volume of 100 μ L were incubated in 96-well plates for 24 h. Next the HeLa cells were infected with 1.5×10^6 bacteria in PBS (multiplicity of infection [MOI] 50:1), which had been obtained from overnight cultures in TSB medium, washed in PBS and resuspended in PBS. The infected HeLa cells were then incubated at 37 °C and 5% CO₂ for 2 h. After 2 h of infection, the plates were washed 3 times with PBS to remove unbound bacteria and, subsequently, lysostaphin (AMBI Products, NY, USA) was added at a final concentration of 20 μ g/mL to eliminate the extracellular bacteria. Incubation was continued for another 2 h, and then 3-(4,5-dimethylthiazol-2-yl)-2,5-diphenyltetrazolium bromide (MTT; Sigma-Aldrich, NL) was added to a final concentration of 0.5 mg/mL to evaluate the viability of the infected HeLa cells. The plates with added MTT were incubated at 37 °C and 5% CO₂ for 3 h. Lastly, the cells were resuspended in 150 μ L of acidic isopropanol, and the absorbance of the suspension was measured at 570 nm. The cytotoxicity of individual *S. aureus* isolates was expressed as the absorbance at 570 nm relative to the control of HeLa cells incubated in the absence of infecting *S. aureus* cells.

Bioinformatic and Statistical Analyses

Bioinformatic tools including TMHMM (version 2.0),²⁶ SignalP (version 4.1),²⁷ LipoP (version 1.0),²⁸ PsortB (version 3.0.2),²⁹ ProtCompB (version 9.0),³⁰ and SecretomeP (version 2.0)³¹ were used for the prediction of subcellular location of proteins identified by MS analyses. Biological processes and

gene annotations were assigned based on the previously annotated *S. aureus* strain NCTC8325, using the AureoWiki database (<http://aureowiki.med.uni-greifswald.de>). To visualize protein functions and the respective protein abundances, Voronoi treemaps were built using Paver version 2.1 (Decodon GmnH, Greifswald, Germany).³² To elucidate relationships between samples of particular groups that had been distinguished based on their exoproteome profiles, correlation coefficients were calculated and principal component analyses were performed on the basis of the MS data using R version 3.4.2.³³ Spearman correlation coefficients were computed with the *cor* function using a pairwise comparison (R package: stats). A *k*-means clustering analysis was performed by clustering the data with the *kmeans* function (R package: stats) and the outcomes were visualized with *fviz_cluster* (R package: factoextra).³⁴ Significant differences in protein spectral counts between isolates belonging to one group were assessed by ANOVA tests (*aov*) and subsequently by the Tukey's Honest Significant Difference (TukeyHSD) method (R package: stats). The statistical significance of differences in the killing of *G. mellonella* larvae by the *S. aureus* t437 Q1–3, a–c subgroups was assessed by Wilcoxon tests and a subsequent Bonferroni correction to adjust the *P*-values using the SAS/STAT software package (version 9.4). The statistical significance of differences in the killing of HeLa cells by the *S. aureus* t437 Q1–3 groups was assessed by ANOVA tests, and a TukeyHSD test was applied for subgroup comparisons using the SAS/STAT software package.

Biological and Chemical Safety

S. aureus is a biosafety level 2 (BSL-2) microbiological agent and was accordingly handled following appropriate safety procedures. All experiments involving live *S. aureus* bacteria and chemical manipulations of *S. aureus* protein extracts were performed under appropriate containment conditions, and protective gloves were worn. All chemicals and reagents used in this study were handled according to the local guidelines for safe usage and protection of the environment.

Data Availability

The mass spectrometry data are deposited in the ProteomeX-change repository PRIDE (<https://www.ebi.ac.uk/pride/>). The data set identifier is PXD009082.

RESULTS

Exoproteome Quantification Distinguishes Three Groups of *S. aureus* t437 Isolates

To identify possible variations in the exoproteomes of previously collected *S. aureus* t437 clinical isolates, we selected 20 different isolates, cultured them in RPMI medium to the stationary phase, and collected the secreted proteins from the growth medium fraction by TCA precipitation. Of note, RPMI medium was used for this study, because previous analyses had shown that the global gene expression profiles of *S. aureus* grown in RPMI medium closely resemble those of *S. aureus* grown in human plasma.³⁵ As can be expected when working with clinical *S. aureus* isolates, we detected some variations in growth among the investigated *S. aureus* isolates, but these related mainly to the lag phase (Figure S1). Further, extracellular proteins were collected in the stationary phase, because the majority of virulence factors are secreted during this particular growth phase.³⁶ Interestingly, the banding patterns of extracellular proteins and their relative intensities

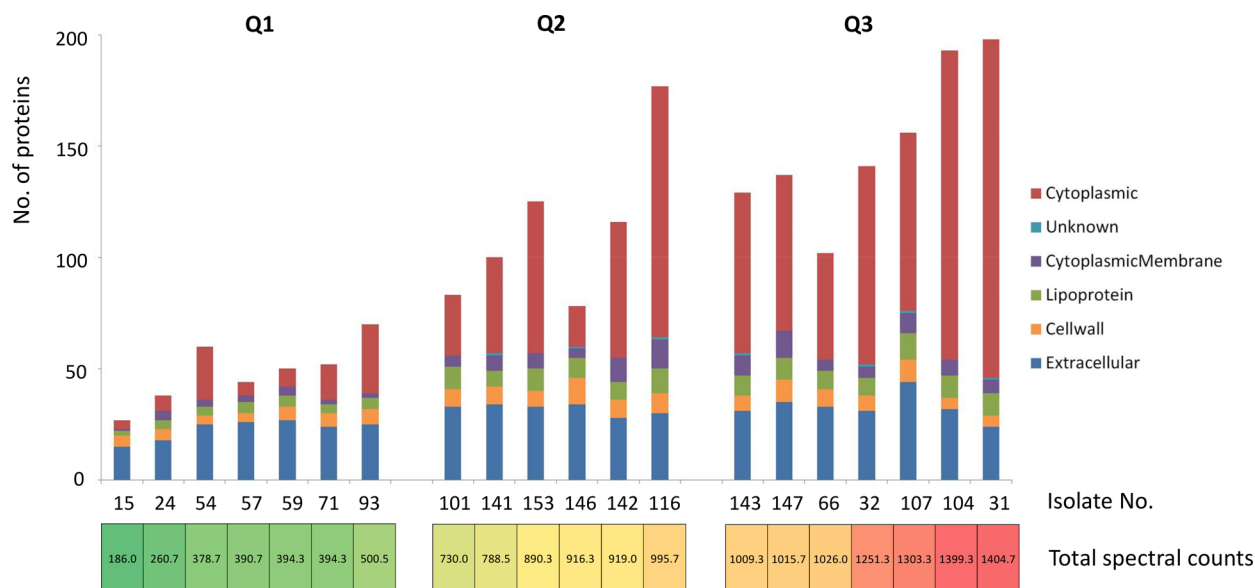


Figure 1. Overview of the numbers of identified extracellular proteins of *S. aureus* t437 isolates and their predicted subcellular locations. On the basis of the numbers of total spectral counts measured for their extracellular proteins, the 20 *S. aureus* t437 study isolates were assigned to three groups designated Q1–3. For each identified extracellular protein, the subcellular location was predicted bioinformatically and the respective numbers of proteins assigned to each subcellular location are indicated in color code. The averaged total numbers of spectral counts measured for the extracellular protein samples from each isolate are presented below the isolate numbers.

showed clear variations in Simply Blue-stained LDS-PAGE gels (Figure S2). This was indicative of exoproteome heterogeneity among the 20 investigated isolates, a notion that was subsequently verified by close inspection of the MS data (Table S2). First, among the total of 303 different identified extracellular proteins, only 23 were found to be shared by all investigated isolates, whereas 102 proteins were uniquely identified for one or two isolates. Second, calculation of total spectral counts revealed substantial variations in the abundance of extracellular proteins between the different isolates, ranging from 186 for isolate 15 to 1404 for isolate 31 (Figure 1). Since this wide range precluded a reliable normalization of total spectral counts, we divided the isolates into three groups (Q1–3) based on the numbers of total spectral counts measured for their extracellular proteins (Table S2). Specifically, the total spectral counts of exoproteins for the Q1 isolates ranged from 186 to 500, for Q2 isolates from 730 to 995, and for Q3 isolates from 1009 to 1404. In accordance with this significant variation, also the total numbers of identified proteins per group differed substantially, ranging between 25 proteins for Q1 (isolate 15) and 198 proteins for Q3 (isolate 31; Figure 1). Further, in the Q1 group, 87 distinct exoproteins were identified for all 7 isolates, while 41.3% of the exoproteins were uniquely identified for one or two strains. In the Q2 group, 50% of the 220 identified proteins were uniquely identified for one or two isolates. In the Q3 group, 36.3% of the 303 identified proteins were unique for all 7 isolates. As an alternative to the initial grouping based on total spectral counts, we verified the clustering of the investigated isolates by the total numbers of identified proteins. This yielded a very similar distribution of the investigated isolates over the Q1–3 groups (Table S3). However, since the total numbers of spectral counts present more information concerning extracellular protein abundance, we decided to use the group classification based on spectral counts for our further analyses. Together, these findings imply that essentially three different exoproteome abundance types can be distinguished among the

20 investigated *S. aureus* t437 isolates. Importantly, this distinction is independent of the country of origin, year of isolation, MLVA type and source (Figure 1, Table 1).

Exoproteome Heterogeneity in *S. aureus* t437 Relates Predominantly to Differential Abundance of Extracellular Cytoplasmic Proteins (ECP)

To assess the nature of the identified proteins, we inspected their predicted subcellular localization with different bioinformatics tools. This showed that the largest level of variation was related to the extracellular appearance of typical cytoplasmic proteins that lack known targeting signals for export from the cytoplasm (Figure 1). The numbers of observed extracellular cytoplasmic proteins were, over all, lowest for the Q1 isolates and highest for the Q3 isolates, ranging from four to 154 (Figure 1). Conversely, differences in the numbers of predicted extracellular proteins with signal peptides for export from the cytoplasm were much smaller. Specifically, for the different isolates, we identified 15–40 typical secretory proteins, 5–12 cell wall-associated proteins, 2–12 lipoproteins, and 1–12 membrane-associated proteins. The observed exoproteome heterogeneity both in terms of identified proteins and their relative abundance based on normalized spectral counts, is reflected in the heat maps for the Q1, Q2, and Q3 groups of isolates presented in Figure 2A and Table S4. These heat maps show that the greatest heterogeneity is observed for exoproteins that are present in relatively low abundance. Intriguingly, typical cytoplasmic proteins appear to be overrepresented in this heterogeneous group of low abundance proteins (Figure 2A). In contrast, the majority of the 30 most abundant extracellular proteins is known to be exported from the cytoplasm with the aid of signal peptides (Figure 2A,B). A representative of the latter class of proteins is the well-characterized immunodominant staphylococcal antigen A (IsaA),^{25,37} which was used to validate the quantitative proteomics data in a Western blot with the aid of a previously developed IsaA-specific monoclonal antibody.³⁸ As

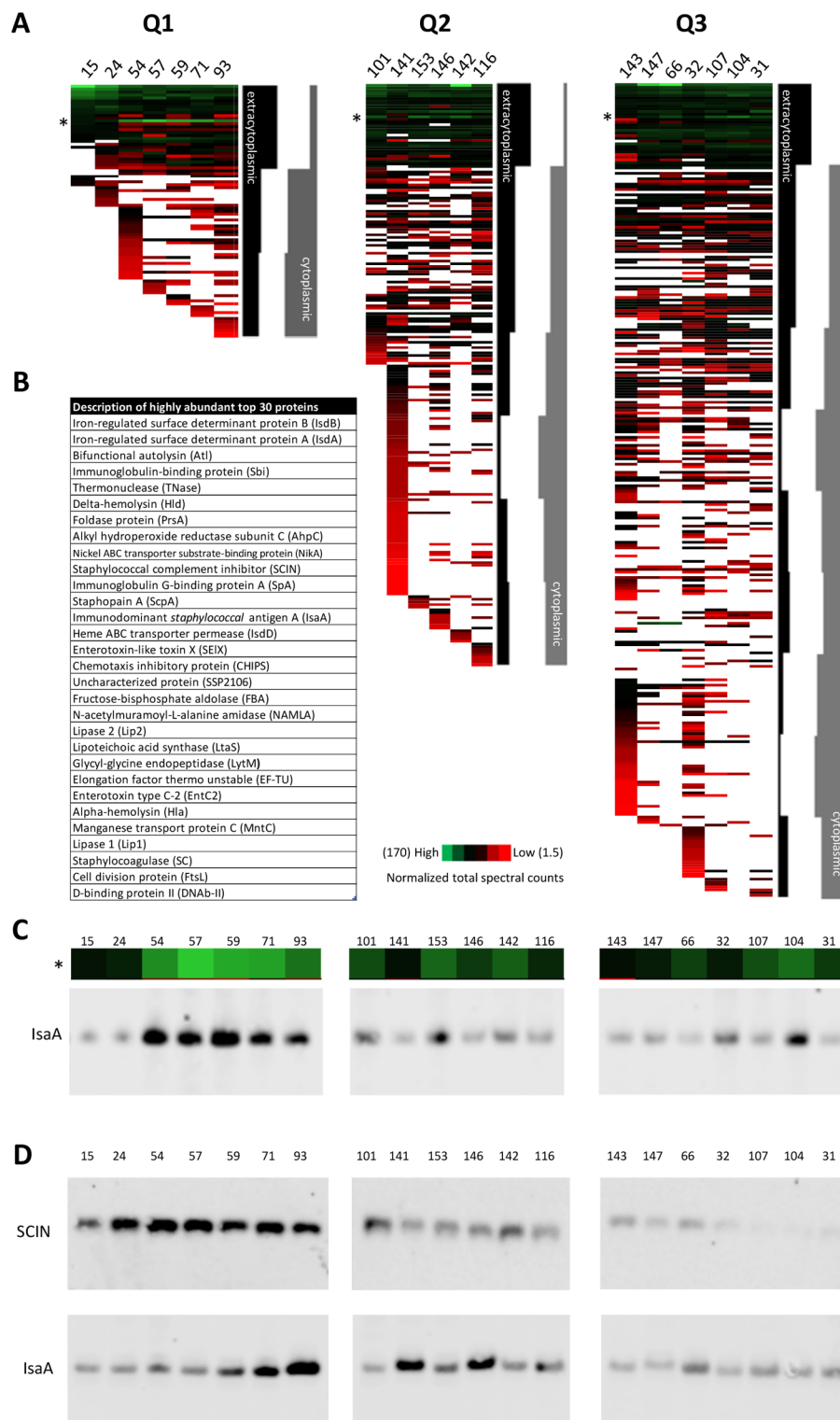


Figure 2. Exoproteome abundance profiles of the investigated *S. aureus* t437 isolates within the Q1–3 groups. (A) Heat-map showing the relative amounts of the identified extracellular proteins within the three Q1–3 isolate groups based on normalized total spectral counts. Color-coded bars within each heatmap represent identified proteins and the isolate numbers are indicated on top of each lane. The black and gray bars flanking each heatmap indicate the relative abundance of extracellular proteins with a predicted cytoplasmic location (gray) versus extracytoplasmic location; each of the respective clusters represents 30 proteins. (B) The 30 most abundant and conserved identified extracellular proteins and their respective descriptions. (C) Comparison of the relative spectral count measurements for IsaA and a Western blot decorated with the monoclonal antibody 1D9 that is specific for IsaA. (D) Protease activity in the growth medium of the investigated *S. aureus* t437 isolates was assessed by assaying the stability of recombinantly produced His₆-tagged IsaA and SCIN proteins added to spent growth medium samples and subsequent Western blotting with His₆-specific antibodies.

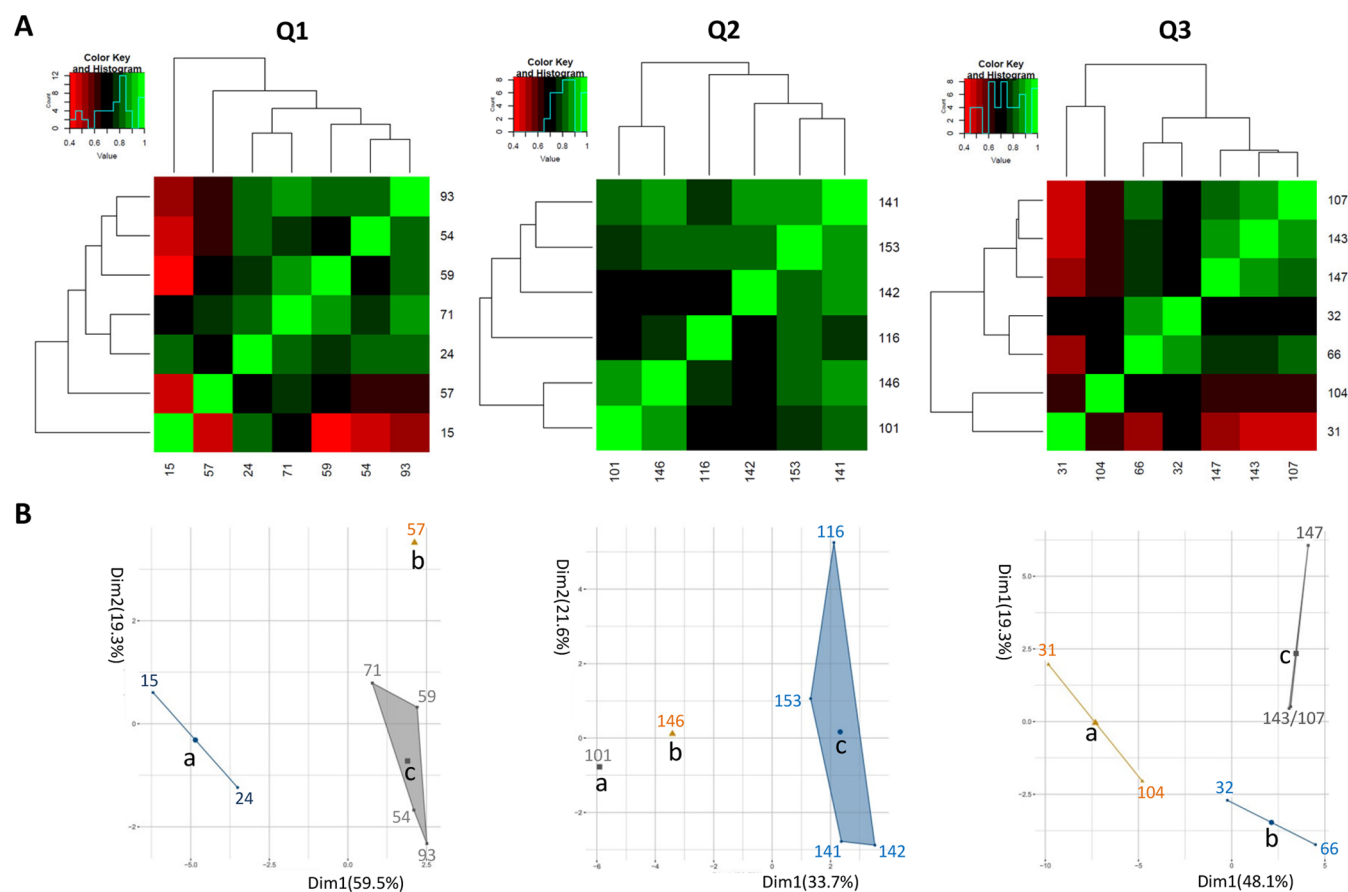


Figure 3. Clustering of isolates within each group based on exoproteome abundance signatures by Spearman correlation and principal component analysis. (A) Spearman correlation of the normalized total spectral counts of identified extracellular proteins within the Q1–3 groups. (B) *k*-means clustering analysis based on the normalized total spectral counts of the identified extracellular proteins. Two-dimensional *k*-means plots further divide each Q-group into three subgroups (a,b,c).

shown in Figure 2C, the relative spectral count measurements for IsaA and the Western blotting data are fully consistent, providing conclusive support for the exoproteome heterogeneity as mapped by mass spectrometry. Together, these observations show that the exoproteome heterogeneity observed for *S. aureus* t437 isolates is largely related to a differential abundance of extracellular cytoplasmic proteins.

It was previously shown for another Gram-positive bacterium, *Bacillus subtilis*, that the appearance of extracellular cytoplasmic proteins can be suppressed by protease activity in the bacterial growth medium.³⁹ To investigate whether proteolytic activity might impact on the extracellular protein abundance, we assessed the possible degradation of the recombinantly produced *S. aureus* proteins IsaA and SCIN in spent media of the 20 investigated *S. aureus* t437 isolates. The advantage of using these proteins as markers for proteolytic activity is that both of them contain a C-terminal His₆ tag that allows their distinction from the respective native proteins secreted by the investigated *S. aureus* isolates. Upon overnight incubation in the spent media at 37 °C, the presence of recombinant IsaA and SCIN was assessed by Western blotting with His₆-specific antibodies. On balance, the highest levels of IsaA and SCIN degradation were observed upon incubation in spent media from isolates of the Q3 group (Figure 2D). This implies that the respective media contain the highest protease levels, which is consistent with the finding that the cysteine protease staphopain A was most abundantly identified in media

of Q3 isolates, and that the zinc metalloprotease aureolysin and the cysteine protease SsaA1 were most abundantly detected in media of Q2 and Q3 isolates (Table S4). In fact, SsaA1 was not detectable in the media of Q1 isolates. This implies that the relatively high abundance of extracellular cytoplasmic proteins in media of the Q3 isolates cannot be correlated to protease activity as was previously shown for *Bacillus*.

S. aureus t437 Groups Q1, Q2, and Q3 Include Subclusters of Isolates with Distinctive Exoproteome Abundance Signatures

To elucidate possible exoproteome relationships among the isolates of each group, Spearman correlation and *k*-means clustering analyses were performed on the basis of protein identifications and the respective protein abundance. For both types of analyses, the normalized total spectral counts of proteins that were produced by all the isolates within each group were used. The Spearman analysis revealed that isolates within the Q2 group are relatively homogeneous with respect to their exoprotein abundance signatures as compared to isolates in the Q1 and Q3 groups (Figure 3A). In the Q1 group, isolate 15 seems relatively less related to the other isolates in this group, and in the Q3 group the same applies for isolate 31. As shown in Figure 3B, the *k*-means clustering analyses provided another angle to elucidate possible exoproteome relationships between isolates, showing that each group of *S. aureus* t437 isolates (Q1–3) can be subdivided into three distinct subgroups (a,b,c). Following

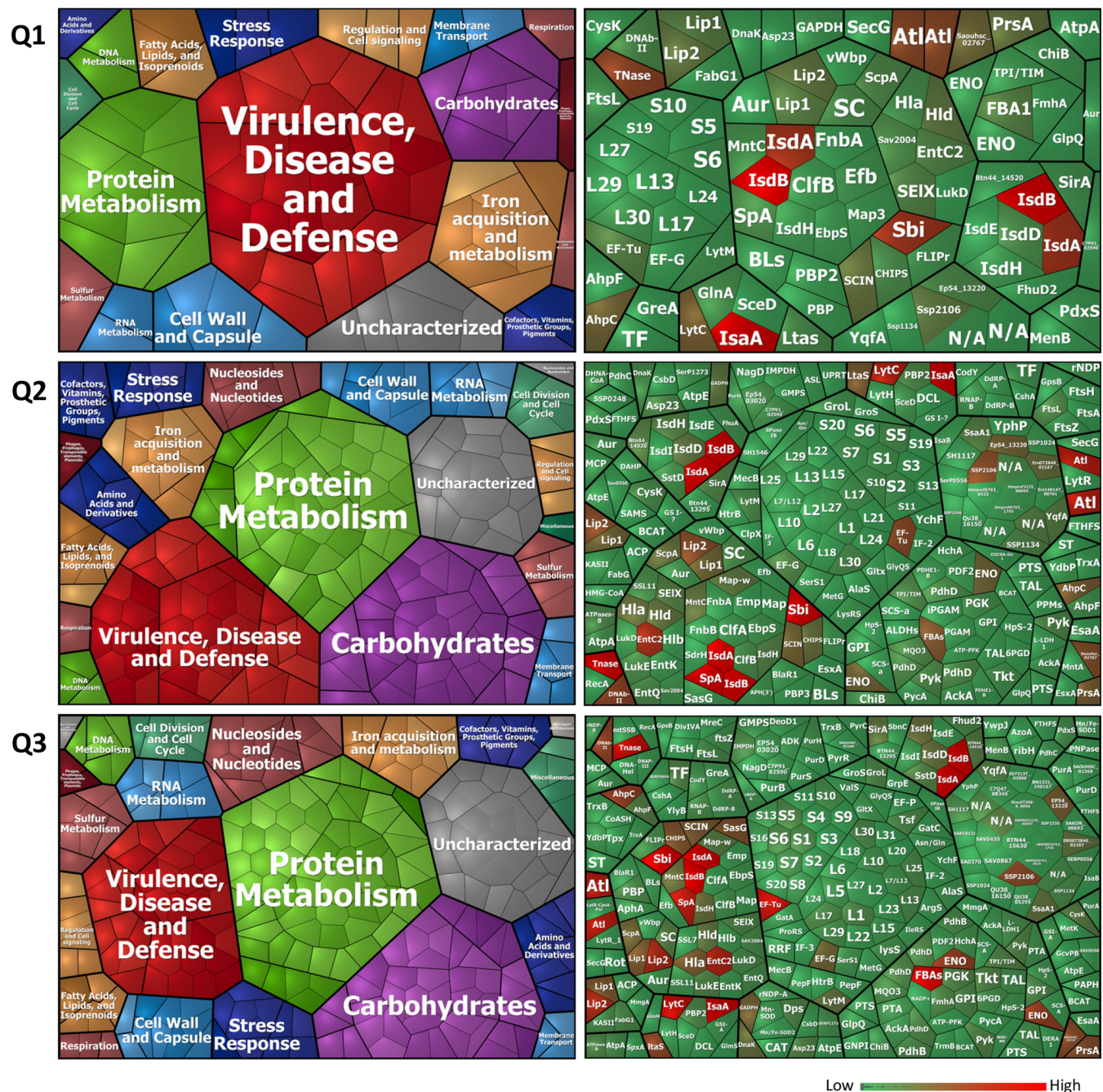


Figure 4. Functional categories and protein functions of identified extracellular proteins within the Q1–3 groups. Voronoi treemaps created with the Paver algorithm show the functional categories assigned to extracellular proteins (left panels) and the respective protein names (right panels) for each Q1–3 group. The different functional categories are marked in different colors, and each protein is represented by a polygon-shaped tile. The size of each category is proportional to the number of identified proteins with the respective functions. In the panels on the right, the relative abundance of each protein is indicated in color code. Of note, particular proteins may have dual functions as exemplified for IsdA and IsdB, which are involved both in iron acquisition and virulence. Accordingly, these proteins are represented twice in the panels on the right.

this subdivision based on differences in protein abundance (as assessed by *k*-means clustering), differences in the number of protein identifications for each subgroup were determined. The Venn diagrams in Figure S3 show the numbers of core and variant extracellular proteins identified for each group. Taken together, the results from these analyses show that each of the Q1–3 groups, which were initially distinguished based on the total spectral counts measured for their exoproteins, is composed of isolates with three different exoproteome abundance signatures.

The Core and Variant Exoproteomes of *S. aureus* t437 Isolates Have Apparently Distinctive Roles in Pathogenesis and Cellular Functions

Despite the heterogeneity observed in the exoproteome profiles of the investigated *S. aureus* t437 isolates, there are nonetheless 30 highly abundant “core” proteins consistently detected ($\geq 80\%$) in the exoproteomes of all three groups of isolates of which about 50% have a role in virulence (Figure 2B). This implies that their dominant expression is characteristic for the core exoproteome of isolates from this particular

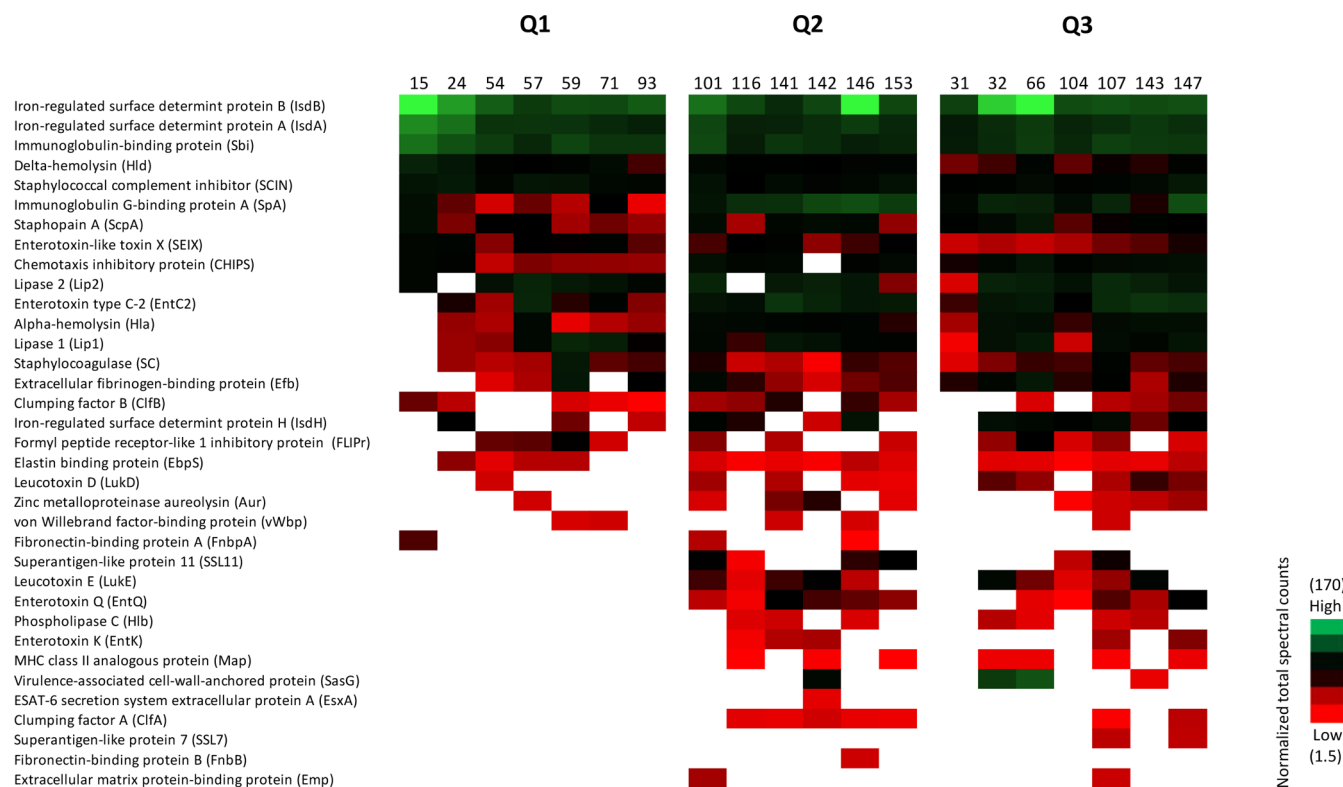


Figure 5. Heat map representation of the relative abundance of identified extracellular virulence factors. A total number of 34 well-known virulence factors was identified for the Q1–3 groups. Color-coded bars within each heatmap represent identified proteins and their relative abundance based on normalized total spectral counts. The isolate numbers are indicated on top of each lane.

staphylococcal lineage. To further zoom in on the collective and variant biological functions of the identified extracellular proteins of the Q1–3 groups, a functional classification based on the annotation of *S. aureus* NTCT8325 was performed using the Paver algorithm. As shown in the Voronoi treemaps presented in Figure 4, the extracellular proteomes of the Q1–3 groups have distinct functional signatures. In particular, 19 different functional categories and 95 predicted protein functions were distinguished for the Q1 group, the most prominently represented functional categories being virulence, disease and defense (30.5%), protein metabolism (13.6%), iron acquisition and metabolism (8.4%), and carbohydrate metabolism (7.3%). For exoproteins of the Q2 group, 20 different functional categories and 240 protein functions were assigned, with protein metabolism (19.5%), virulence, disease, and defense (18.3%), carbohydrate metabolism (16.6%), and iron acquisition and metabolism (4.5%) being the most prominent categories. For exoproteins of the Q3 group, 21 functional categories and 308 predicted protein functions were assigned, with protein metabolism (21.1%), carbohydrates metabolism (14.9%), virulence, disease, and defense (13.8%), and nucleosides and nucleotides (5.6%) being most prominent. Altogether, the observations presented in Figures 2A,B and 4 imply that, over all, the core and variant exoproteomes of the investigated *S. aureus* t437 isolates have apparently distinctive roles in pathogenesis and cellular functions.

Production of Known Virulence Factors by *S. aureus* t437 Isolates Is Highly Heterogeneous

Our exoproteome analyses identified in total 35 proteins implicated in staphylococcal virulence. The relative abundance of these known virulence factors as produced by the individual

investigated isolates is represented in Figure 5. Twelve of these proteins are primarily linked with bacterial adhesion to cells and tissues of the human host, including three iron-regulated surface determinants (IsdA, IsdB, IsdH), six proteins belonging to the so-called “microbial surface components recognizing adhesive matrix molecules” (MSCRAMM) family (ClfA, ClfB, EbpS, Emp, FnbpA, FnbpB, Map, SpA, and vWbp), and SasG. Eighteen identified virulence factors are secreted proteins that serve to disrupt host cells and promote spreading, including five exoenzymes (Aur, Lip1, Lip2, SC, and ScpA), five cytolytic toxins (Hla, Hlb, Hld, LukD, and Luke), six superantigens (EntC2, EntK, EntQ, SEIX, SSL7, and SSL11), and EsxA. In addition, we identified five proteins (CHIPS, Efb, FLIPr, Sbi, and SCIN), which are involved in the evasion of innate or adaptive immune responses of the host. As shown in Figure 5, the expression of these 35 virulence factors by *S. aureus* t437 isolates was highly heterogeneous in the different groups of isolates. In particular, isolates belonging to the Q1 group produced on average less known virulence factors than isolates belonging to the other two groups.

Subclustering of *S. aureus* t437 Isolates Based on Normalized Total Spectral Counts of Exoproteins Is Predictive for High or Low Rates of Killing in a Larval Infection Model

The observed differences in the production of known virulence factors by the different *S. aureus* t437 isolates was suggestive of possible differences in the virulence of these isolates. Therefore, we assayed their virulence using a *Galleria mellonella* larval infection model, where the bacteria are solely challenged by innate immune defenses.¹⁸ Specifically, each of the 20 investigated *S. aureus* t437 isolates was used to infect 15

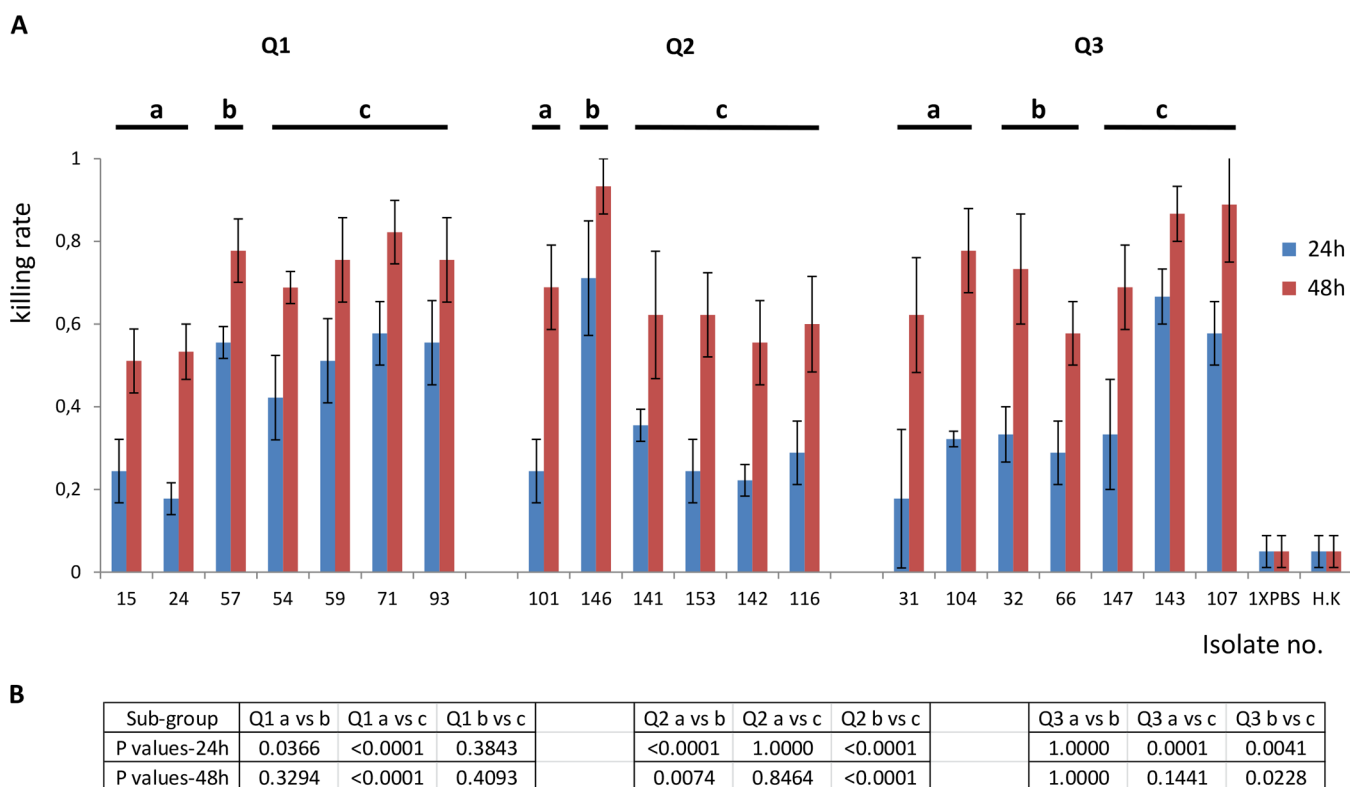


Figure 6. Virulence of the 20 investigated *S. aureus* t437 isolates in a *G. mellonella* infection model. (A) Larvae of *G. mellonella* were inoculated with 2.5×10^6 CFUs of the 20 *S. aureus* t437 study isolates. Killing of the larvae was assessed at 24 and 48 h post inoculation. All values are the mean \pm the standard deviation of three independent infection experiments. HK, heat-killed bacteria. (B) Statistical significance of observed differences in virulence between the identified *S. aureus* t437 subgroups as assessed using a Wilcoxon test. A *P*-value <0.05 was considered significant.

Table 2. Extracellular Proteins of *S. aureus* t437 Isolates Significantly or Uniquely Associated with High or Low Virulence in the *Galleria mellonella* Infection Model^a

Q1 a versus b and c	Iron-regulated surface determinant protein B (IsdB)	a \uparrow	b and c \downarrow	(<i>P</i> < 0.0001)
	Iron-regulated surface determinant protein A (IsdA)	a \uparrow	b and c \downarrow	(<i>P</i> = 0.0002)
	Immunodominant staphylococcal antigen A (IsaA)	a \downarrow	b and c \uparrow	(<i>P</i> < 0.0001)
	Chitinase B (ChiB)	a-	b and c+	
	<i>N</i> -Acetylmuramyl-L-alanine amidase (Sle1)	a-	b and c+	
Q2 b versus a and c	Iron-regulated surface determinant protein B (IsdB)	b \uparrow	a and c \downarrow	(<i>P</i> < 0.0001)
	Elongation factor G (EF-G)	b-	a and c+	
	Pyruvate kinase (PK)	b-	a and c+	
	Pyruvate dehydrogenase E1 component subunit alpha (PDHA1)	b-	a and c+	
	High-affinity heme uptake system protein (IsdE)	b+	a and c-	
	Extracellular fibrinogen binding protein (Efb)	b+	a and c-	
	ATP synthase subunit beta (ATPases)	b-	a and c+	
	30S ribosomal protein (S10)	b-	a and c+	
	ATP synthase subunit alpha (ATPases)	b-	a and c+	
	1,4-Dihydroxy-2-naphthoyl-CoA synthase (DHNA-CoA)	b-	a and c+	
Q3 c versus a and b	Ser-Asp rich fibrinogen/bone sialoprotein-binding protein (SdrH)	b+	a and c-	
	Fibronectin-binding protein B (FnBB)	b+	a and c-	
	Chitinase B (ChiB)	c+	a and b-	
	50S ribosomal protein (L7/L12)	c-	a and b+	
	50S ribosomal protein (L5)	c-	a and b+	

^aStatistical significance in the amounts of particular extracellular proteins per Q1–3 group and the respective a,b,c subgroups was assessed by ANOVA; “ \uparrow ”, indicates a significantly higher level of protein abundance and “ \downarrow ” a significantly lower protein abundance level. Proteins consistently present or absent in the respective groups and subgroups are indicated with “+” or “-”, respectively.

larvae, where a bacterial suspension of 10 μ L containing 2.5×10^6 CFUs in PBS was used per larval inoculation. Subsequently, the larval mortality was assessed at 24 and 48 h post infection (p.i.). As a control, larvae were inoculated with

heat-killed bacteria equivalent to 2.5×10^7 CFU prior to heat inactivation (i.e., a 10-fold higher CFU count than used in inoculations with living bacteria). The vast majority of larvae inoculated with heat-killed bacteria survived for 48 h p.i.

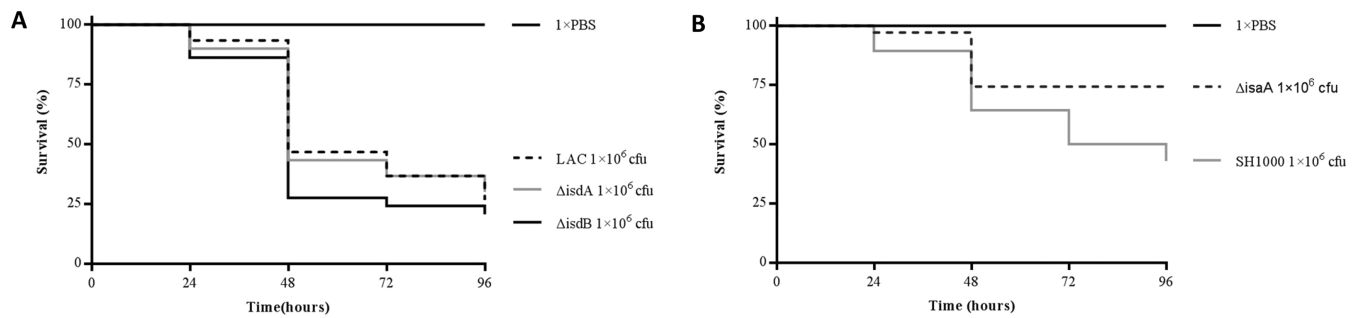


Figure 7. Assessment of possible roles of IsdA, IsdB, and IsaA in staphylococcal virulence in a *G. mellonella* infection model. (A) Effect of the inoculation of *G. mellonella* larvae ($n = 30$) with 1×10^6 CFUs of *S. aureus* USA300 LAC, or *isdA* or *isdB* mutant derivatives of this strain on larval survival. (B) Effect of the inoculation of *G. mellonella* larvae ($n = 30$) with 1×10^6 CFUs of *S. aureus* SH1000 or an *isaA* mutant derivative of this strain on larval survival. The survival rates were monitored from 24 to 96 h post infection. The statistical significance of the observed differences was assessed using a Wilcoxon test. A P -value < 0.05 was considered significant (*isdA* vs wild-type, $P = 0.8621$; *isdB* vs LAC, $P = 0.1642$; *isaA* vs SH1000, $P = 0.0325$).

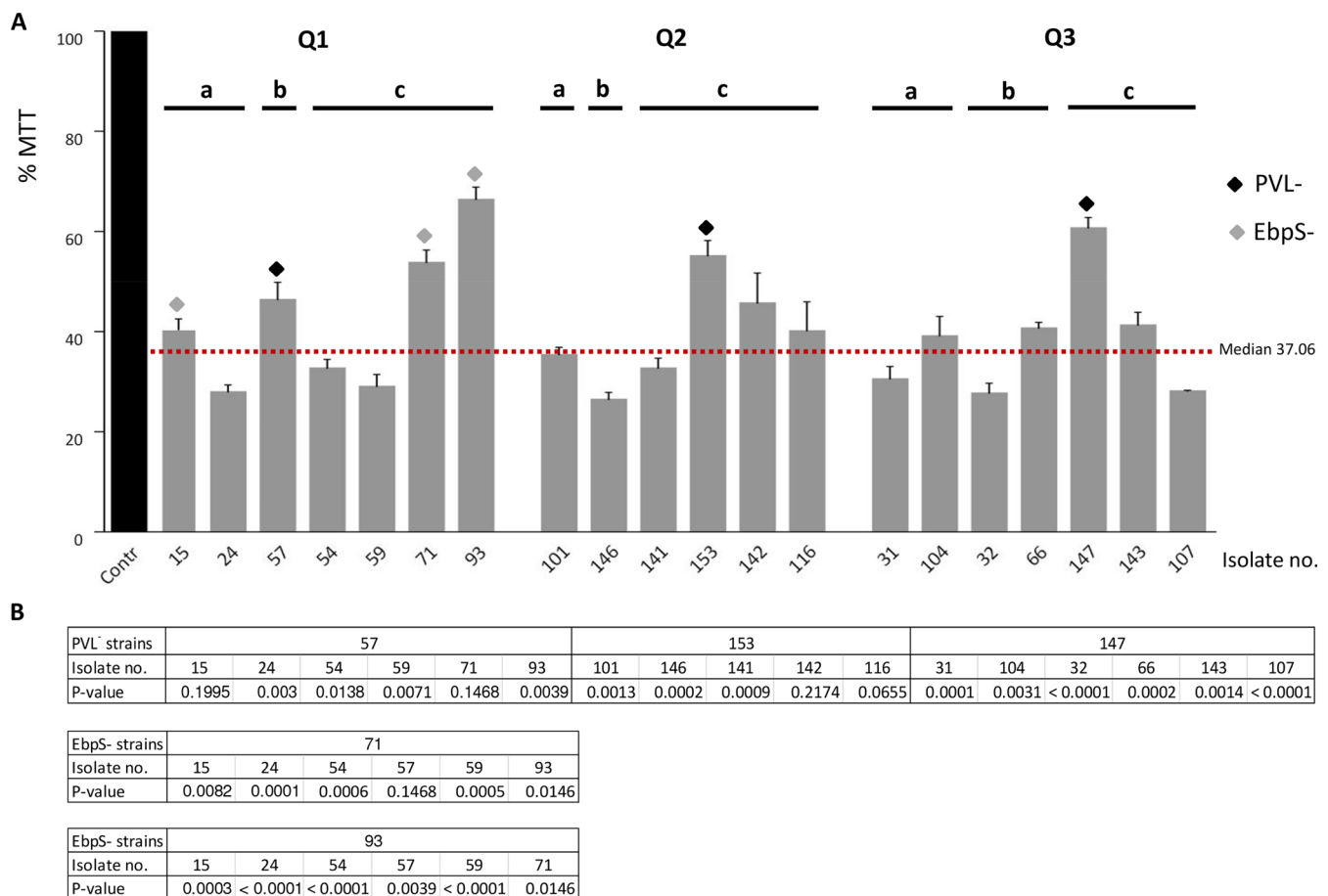


Figure 8. Cytotoxicity of the 20 investigated *S. aureus* t437 isolates in a HeLa cell infection model. (A) HeLa cells were infected with bacteria at a MOI of 50:1. Upon 2 h incubation, lysostaphin was added to eliminate the extracellular bacteria. After another 2 h incubation, MTT was added to evaluate the viability of the infected HeLa cells. The results are shown as the percentage of MTT reduction relative to the uninfected control. (B) The statistical significance of differences in the killing of HeLa cells by *S. aureus* t437 PVL- or EbpS-negative isolates was assessed by t tests. Please note that the absence of PVL from particular strains was previously demonstrated (Table 1), and that the EbpS-negative designation relates to a lack of identification of EbpS in the present exoproteome analysis. P -values < 0.05 were considered significant. The P -values for isolate 15 versus isolates 24, 54, and 59 are 0.0036, 0.0369, and 0.0149, respectively.

(Figure 6). In contrast, inoculation with living bacteria resulted in death of the majority of larvae within 48 h p.i. Between different *S. aureus* t437 isolates, the largest variations in larval killing were observed at 24 h p.i., while differences in the larval killing rates at 48 h p.i. were relatively smaller. For example, inoculation with bacteria from the Q1 group resulted in

average killing rates between 17.7% (strain Q1–24) and 57.7% (strain Q1–71) at 24 h p.i. At 48 h p.i. the larval killing due to inoculation with isolates from the Q1 group ranged between 51.1% (strain Q1–15) and 77.7% (strain Q1–71). Similar larval killing rates were observed upon inoculation with *S. aureus* t437 isolates from groups Q2 and Q3. Of note, the

observed variations could not be correlated to geographical regions where the *S. aureus* isolates had been collected, different host environments, or particular MLVA types (Table 1). However, for *S. aureus* isolates from the Q1, Q2, and Q3 groups, a clear correlation between the larval killing rates and the *k*-means clustering-based separation of isolates into different subclusters was observed. In particular, isolates from the Q1a, Q2a, Q2c, Q3a, and Q3b subclusters displayed relatively low-level killing of larvae (i.e., <40% killing at 24 h p.i.), while isolates from the Q1b, Q1c, and Q2b subclusters showed relatively high rates of larval killing (Figure 6; Table S5). Only among isolates from the Q3c subcluster we observed both high and low rates of larval killing.

To investigate which extracellular proteins might be involved in the differences in larval killing activity per “Q-group”, we assessed the statistically significant differences in the abundance, as well as the presence or absence, of particular exoproteins in the respective subclusters with high or low killing activity. This revealed that distinguishing features for Q1 isolates with high killing activity (subclusters Q1b and Q1c) were the production of a secreted Chitinase B (ChiB) and the amidase Sle1, relatively high levels of IsaA, and relatively low levels of the IsdA and IsdB proteins (Table 2). Interestingly, also for isolates from the Q3 group with mostly high killing activity (Q3c), the identification of Chitinase B was a distinguishing feature. Distinguishing features of isolates with high killing activity in the Q2 group (i.e., subcluster Q2b) were relatively high levels of IsdB, and the unique identification of Efb, FnbB, IsdE, and SdrH (Table 2). To verify possible effects of some of these extracellular proteins on virulence, we tested *isdA*, *isdB*, or *isaA* mutant strains along with the respective parental strains in the *G. mellonella* infection model. Compared to the wild-type, the *isdA* and *isdB* mutations in the *S. aureus* USA300 LAC background displayed no significant differences in larval killing (Figure 7A), whereas the rate of larval killing by the investigated *isaA* mutant was significantly lower compared to the respective *S. aureus* SH1000 wild-type (Figure 7B). Taken together, these observations imply that the *k*-means clustering analysis based on the normalized total spectral counts of exoproteins that were produced by all the isolates within each Q group distinguishes those isolates that show comparable levels of virulence, at least in the *G. mellonella* infection model.

***S. aureus* t437 Isolates Show Relatively Small Variations in Cytotoxicity in a HeLa Cell Infection Model**

The observed differences in the larval killing activity by the different *S. aureus* t437 isolates mostly reflect the ability of the respective bacteria to survive a challenge by professional phagocytes of *G. mellonella*. This prompted us to also investigate their ability to invade and kill nonprofessional phagocytic cells. To this end, we applied HeLa cells, which were exposed to *S. aureus* at a MOI of 1:50. After 2 h, lysostaphin was added to eliminate the extracellular, non-internalized bacteria and an MTT activity assay was applied to evaluate the viability of the infected HeLa cells. The results are presented in Figure 8 as the percentage of MTT activity relative to that of the uninfected control cells. Interestingly, although some variations in the killing of HeLa cells were observed, the differences were mostly not significant (Figure 8B; Table S5). Of note, as shown in Figure 8A, a relatively low cytotoxicity was observed for three Pantone-Valentine Leukocidin (PVL)-deficient isolates (i.e., 57, 147, 153; Table 1), and

three isolates that seem to lack the adhesin EbpS as judged by the present exoproteome analysis (i.e., 15, 71, and 93; Figure 5). Thus, the substantial differences observed for the exoproteomes of the investigated *S. aureus* t437 isolates are not mirrored in the ability to invade and kill nonprofessional phagocytic HeLa cells.

DISCUSSION

In the present study, we have performed a first comparative exoproteome profiling analysis for *S. aureus* with the *spa*-type t437, including 20 isolates from eight different countries. In a previous study, we described this clone as a genetically tight cluster belonging to the CC59 clonal complex.⁸ Nonetheless, our analysis uncovered substantial exoproteome heterogeneity among these strains, and only relatively few proteins were found to be produced by all investigated isolates. In contrast, a large number of proteins was found to be unique for one or two strains under the conditions tested. Of note, we have previously uncovered substantial exoproteome heterogeneity for the *S. aureus* species by investigating clinical isolates derived from one hospital, but belonging to different clonal lineages.¹⁵ This was attributed to the large plasticity of the *S. aureus* genome, which is continuously reshaped by the acquisition and loss of mobile genomic elements, as well as strain-specific differences in gene expression, translation, protein secretion and post-translational protein modifications.⁴⁰ On the other hand, we demonstrated more recently that the exoproteomes of *S. aureus* USA300 isolates from the Copenhagen area in Denmark display fairly homogeneous exoproteomes, of which the composition could be associated with their epidemicity.⁴¹ This appears to be different for the closely related *S. aureus* t437 isolates in our present study, which were collected in different European countries and China. Although it is suggestive that the geographical distribution could play a role in the observed exoproteome heterogeneity, it was not possible to associate particular exoproteome profiles to particular countries or even to particular subtypes of *S. aureus* t437 as distinguished by MLVA or MultiLocus Variable-number tandem repeat Fingerprinting. A similar observation was reported by Liew et al., who compared pairs of *S. aureus* isolates belonging to ST1, ST8 and ST33.⁴² To date, it was difficult to explain this exoproteome heterogeneity. Importantly, however, our present data do shed light on possible underlying mechanisms, in particular because a large extent of the observed variation relates to the release or excretion of typical cytoplasmic proteins, whereas the variations observed for proteins secreted with the aid of Sec-type signal peptides were relatively small.

In addition to proteins which are actively exported from the cytoplasm via different secretion systems, the Sec system in particular, the exoproteomes of *S. aureus* and many other bacteria contain large numbers of typical cytoplasmic proteins (Table S6).^{43,44} Consequently, the numbers of detectable extracellular proteins of *S. aureus* may become very large as exemplified by >1300 exoprotein identifications in a recent study.⁴⁵ The mechanisms by which these proteins are released from the cytoplasm have been enigmatic for a long time. However, in recent years a general picture has emerged where this so-called alternative secretion⁴⁶ or excretion of cytoplasmic proteins (ECP)⁴⁷ is the end result of different processes, involving cell lysis caused by autolysins,⁴⁸ phage activity, the production of cytolytic toxins,⁴⁹ and/or proteolytic activity.⁵⁰ In the present study, we observed a massive variation in the

amounts of extracellular proteins to the extent that we had to distinguish three groups (i.e., Q1, Q2, and Q3) based on the total number of spectral counts of extracellular proteins detected by MS. Interestingly, the variation in ECP could not be correlated to the production of the major autolysin Atl, which was detectable in comparable amounts in the exoproteomes of the different isolates (Table S4). On the other hand, we did observe a phage coat protein in the exoproteomes of isolates belonging to groups Q2 and Q3 that displayed high levels of ECP. In addition, among the exoproteomes of these isolates we detected the phospholipase C, which is encoded by the *hlyB* gene into which the so-called β -hemolysin-converting bacteriophages are usually integrated.⁵¹ Such phages encode immune evasion factors, like SCIN and CHIPS, which were abundantly detected in the exoproteomes of the here investigated *S. aureus* t437 isolates. Hence, we consider it likely that the observed exoproteome heterogeneity in groups Q2 and Q3 can be attributed at least to some extent to (pro)phage activity. Intriguingly, we detected higher amounts of the extracellular protease staphopain A in media of Q3 isolates, and of the proteases aureolysin and SsaA1 in media of Q2 and Q3 isolates, where the Q3 isolates show the highest levels of ECPs. This is different from the situation encountered in *B. subtilis* where overproduction of secreted proteases led to complete degradation of ECPs, whereas the deletion of multiple genes for secreted proteases led to highly increased levels of ECPs.^{39,52} The latter was due both to decreased turnover of ECPs and enhanced autolysin activity as secreted proteases are needed to control autolysin activity. Likewise, a recent study using *S. aureus* USA300 LAC showed that increased protease production due to a *sarA* mutation resulted in a substantial reduction in the number of identified extracellular proteins.⁴⁵ Thus, despite the fact that extracellular proteases have been described as modulators of virulence factor stability,⁵³ it seems that other mechanisms like prophage activity are more dominant in the appearance of ECPs in the investigated *S. aureus* t437 isolates.

Irrespective of the precise mechanisms underlying ECP, it has become increasingly clear that certain cytoplasmic proteins can play decisive roles in host colonization and infection. These multifunctional proteins are usually described as “moonlighting proteins”. In many cases, moonlighting proteins are evolutionarily well-conserved metabolic enzymes or molecular chaperones.⁵⁴ For instance, glyceraldehyde-3-phosphate dehydrogenase (GAPDH), the first identified moonlighting bacterial enzyme, was found to serve not only as a glycolytic enzyme in the cytoplasm, but also as a virulence-enhancing protein when associated with the cell surface of pathogenic streptococci.⁵⁵ In the exoproteomes of the *S. aureus* t437 lineage, we identified 3 well-known moonlighting proteins, namely fructose-bisphosphate aldolase, alkyl hydroperoxide reductase and elongation factor Tu. In fact, all investigated isolates showed relatively high extracellular levels of these three proteins. The cytoplasmic form of fructose-bisphosphate aldolase is a glycolytic enzyme but, upon ECP by *Candida albicans* and *Neisseria meningitidis*, this protein was shown to be involved in plasminogen binding and adhesion to human cells.^{56,57} The alkyl hydroperoxide reductase is generally responsible for detoxification of reactive oxygen species, but it was also implicated in heme-binding by *Streptococcus agalactiae*.⁵⁸ The cytoplasmic form of elongation factor Tu catalyzes the binding of aminoacyl-tRNA to the ribosome but, when exposed on the surface of *Mycoplasma*

pneumoniae and *Streptococcus gordonii*, it can also play roles in fibronectin- and mucin-binding, respectively.^{59,60} It thus seems that the release of cytoplasmic proteins into the extracellular environment, either by lysis or other mechanisms, can be regarded as an altruistic mechanism for the bacterial population. On this basis, it can be anticipated that several of the presently identified ECPs may serve additional roles in host colonization and infections caused by *S. aureus* t437.

One of the major challenges in understanding and predicting the virulence of *S. aureus* is imposed by the multitude of virulence factors produced by this pathogen, all of them serving different but sometimes overlapping, redundant or even synergistic roles during different stages of infection. Accordingly, it has thus far been close to impossible to correlate clinical data to particular exoproteome profiles. We therefore made a first attempt to correlate our exoproteome data to bacterial virulence in a simple high-throughput animal model involving the larvae of *Galleria mellonella*. Of note, in this model bacteria are injected into the larvae, which means that early stages in the infection process, like adhesion, colonization and breakage of barriers for infection are bypassed. Instead, the bacteria are directly confronted by the innate immune response of the larvae.¹⁸ Furthermore, for a number of opportunistic human pathogens good correlations were observed between infection of mice and *G. mellonella*.^{61,62} Importantly, the *Galleria* model has already been successfully applied in the identification of virulence factors of *S. aureus*, and the efficacy of anti-staphylococcal agents.^{63,64} Intriguingly, we observed that particular quantitative proteomic signatures within each Q-group of investigated *S. aureus* t437 isolates correlated well with high or low virulence in the *Galleria* model, irrespective of the numbers of different extracellular proteins produced. Instead, certain proteins such as IsaA, IsdB, IsdA, IsdE, IsdH, and Chitinase B could be related to the observed killing of larvae. For instance, the housekeeping protein IsaA, which has been identified as a major antigen of *S. aureus* and a potential candidate for antibody-based therapy,⁶⁵ was a distinctive feature of the exoproteome profile of the highly virulent subgroups Q1b and Q1c. Consistent with this notion, an *isaA* deletion mutant was found to be attenuated in the *G. mellonella* infection model. A role of IsaA in staphylococcal virulence had not yet been reported, but it would in fact explain why this protein is invariably produced in all investigated clinical *S. aureus* isolates.^{15,66} Also, the hydrolytic enzyme Chitinase B was uniquely present in the exoproteomes of the highly virulent subgroups Q1b, Q1c, and Q3c. The impact of the latter enzyme could in principle be due to the degradation of larval chitin.⁶⁷ However, it has to be noted that chitin and chitinases were previously proposed to serve as important regulators of innate and adaptive immune responses.⁶⁸ It is thus conceivable that the produced Chitinase B also serves a function in immune evasion and infection, not only in the *Galleria* model, but even in the human body from which all investigated *S. aureus* t437 isolates included in our study were originally derived. Clearly, this will require further in-depth analyses. Confidence that the observed exoproteome abundance profiles may be meaningful for virulence of the investigated *S. aureus* isolates can be derived from the fact that multiple proteins involved in iron homeostasis were found to be associated with virulence, albeit in a differential manner. The latter may explain why we did not observe a distinctive effect of individual *isdA* or *isdB* mutations on virulence in the *G. mellonella* model. Nonetheless, the importance of iron

homeostasis determinants for virulence would be consistent with the fact that both humans and *G. mellonella* represent an iron restricted environment for *S. aureus*, where iron deprivation may impose a need for high virulence whereas a good ability to acquire iron may to some extent obviate the need to be virulent. Thus, the fact that we can correlate certain *S. aureus* t437 exoproteome abundance profiles to high or low virulence in the *G. mellonella* model implies that these profiles may also be relevant for the potential to cause infection in particular niches of the human body. In this respect, one has to bear in mind that animal models, such as the larvae of *G. mellonella*, reflect the human setting only partially. Furthermore, different bacterial traits are required to infect different niches in the human body. Consistent with this view, the investigated *S. aureus* t437 isolates behaved differently in the HeLa cell infection model, where we essentially assayed their ability to invade and kill nonprofessional phagocytic cells. In the latter infection scenario, it appears that the presence or absence of the adhesin EbpS or the toxin PVL may have a greater impact on the viability of infected host cells than the major differences that we observed in the composition of the exoproteomes of the individual investigated *S. aureus* t437 isolates.

CONCLUSION

The present study provides a detailed survey of the extracellular proteome and virulence assessment of the *S. aureus* lineage with *spa*-type t437. The results allowed a separation of 20 representative clinical isolates into three groups and nine subclusters with different exoproteome abundance profiles. This shows that, despite the high degree of genomic relatedness within this lineage, its exoproteome is highly heterogeneous. This has important bearings on the virulence of these isolates as was shown using a *G. mellonella* larval infection model. On the other hand, the virulence of the investigated isolates as assayed in the HeLa cell toxicity assay most likely mirrors the relatively few variations observed for a core set of about 20 known extracellular virulence factors that typify the *S. aureus* t437 lineage. Here one has to bear in mind that *S. aureus* requires different virulence factors to invade, thrive, and survive in different niches of the human body. Thus, the present data provide novel leads for further dissection of the roles of particular exoproteome profiles or individual extracellular proteins in staphylococcal virulence.

ASSOCIATED CONTENT

Supporting Information

The Supporting Information is available free of charge on the ACS Publications website at DOI: [10.1021/acs.jproteome.9b00179](https://doi.org/10.1021/acs.jproteome.9b00179).

Figure S1: Growth curves of investigated *S. aureus* t437 isolates; Figure S2: LDS-PAGE of the extracellular proteins of the investigated *S. aureus* t437 isolates; Figure S3: Venn diagrams summarizing total numbers of identified extracellular proteins in the Q1–3 groups of investigated *S. aureus* t437 isolates (PDF)

Table S1: Proteins identified by mass spectrometry and numbers of spectral counts for each protein per replicate (XLSX)

Table S2: Total spectral counts of the identified proteins and distinction of the Q1, Q2, and Q3 isolate groups

based on the total numbers of spectral counts measured for their extracellular proteins (XLSX)

Table S3: Comparison of *S. aureus* t437 isolate clustering based on total spectral counts (A) or total identified proteins (B) (XLSX)

Table S4: Identified extracellular proteins, predicted subcellular locations, molecular weights, and heatmap of normalized spectral counts (XLSX)

Table S5: Statistical analysis of differences in the virulence of *S. aureus* t437 Q1, Q2, and Q3 subgroups (a,b,c) in the *G. mellonella* and HeLa cell infection models (XLSX)

Table S6: Overview of extracellular cytoplasmic proteins (ECP) identified in the exoproteomes of *Bacillus* species and *Streptococcus pyogenes* (XLSX)

AUTHOR INFORMATION

Corresponding Author

*E-mail: j.m.van.dijl01@umcg.nl

ORCID

Xin Zhao: 0000-0002-5392-1749

Dörte Becher: 0000-0002-9630-5735

Jan Maarten van Dijl: 0000-0002-5688-8438

Author Contributions

#X.Z. and L.M.P.M. contributed equally.

Notes

The authors declare no competing financial interest. The mass spectrometry data are deposited in the ProteomeX-change repository PRIDE (<https://www.ebi.ac.uk/pride/>). The data set identifier is PXD009082.

ACKNOWLEDGMENTS

We thank Jia Zhang, Min Wang, and Yanyan Fu for support with the statistical analyses. This work was funded by the China Scholarship Council (grant 201506170036 to X.Z.), the Graduate School of Medical Sciences of the University of Groningen (to X.Z., L.M.P.M., T.S., C.G., and J.M.v.D.), the Faculty of Science and Engineering of the University of Groningen (to A.d.J., P.U., R.S., and W.J.Q.), and the Deutsche Forschungsgemeinschaft Grant GRK1870 (to L.M.P.M. and D.B.).

ABBREVIATIONS

ACN, acetonitrile; BSL-2, biosafety level 2; CC, clonal complex; CFU, colony forming units; DTT, dithiothreitol; ECP, extracellular cytoplasmic proteins; IAA, iodoacetamide; LDS, lithium dodecyl sulfate; MLST, multilocus sequence typing; MLVA, multiple-locus variable number tandem repeat analysis; MRSA, methicillin-resistant *S. aureus*; MS, mass spectrometry; MTT, 3-(4,5-dimethylthiazol-2-yl)-2,5-diphenyltetrazolium bromide; OD₆₀₀, optical density at 600 nm; PBS, phosphate-buffered saline; RPMI, Roswell Park Memorial Institute 1640 medium; ST, sequence type; TCA, trichloroacetic acid; TFA, trifluoroacetic acid; TSB, tryptic soy broth.

REFERENCES

- (1) Wertheim, H. F. L.; Melles, D. C.; Vos, M. C.; van Leeuwen, W.; van Belkum, A.; Verbrugh, H. A.; Nouwen, J. L. The role of nasal carriage in *Staphylococcus aureus* infections. *Lancet Infect. Dis.* **2005**, *5*, 751–762.

- (2) Nannini, E.; Murray, B. E.; Arias, C. A. Resistance or decreased susceptibility to glycopeptides, daptomycin, and linezolid in methicillin-resistant *Staphylococcus aureus*. *Curr. Opin. Pharmacol.* **2010**, *10*, 516–521.
- (3) Song, J. H.; Hsueh, P. R.; Chung, D. R.; Ko, K. S.; Kang, C. I.; Peck, K. R.; Yeom, J. S.; Kim, S. W.; Chang, H. H.; Kim, Y. S.; et al. Spread of methicillin-resistant *Staphylococcus aureus* between the community and the hospitals in Asian countries: an ANSORP study. *J. Antimicrob. Chemother.* **2011**, *66*, 1061–1069.
- (4) Ho, C. M.; Ho, M. W.; Lee, C. Y.; Tien, N.; Lu, J. J. Clonal spreading of methicillin-resistant SCCmec *Staphylococcus aureus* with specific spa and dru types in central Taiwan. *Eur. J. Clin. Microbiol. Infect. Dis.* **2012**, *31*, 499–504.
- (5) Ko, K. S.; Lee, J. Y.; Suh, J. Y.; Oh, W. S.; Peck, K. R.; Lee, N. Y.; Song, J. H. Distribution of major genotypes among methicillin-resistant *Staphylococcus aureus* clones in Asian countries. *J. Clin. Microbiol.* **2005**, *43*, 421–426.
- (6) Yang, X.; Qian, S.; Yao, K.; Wang, L.; Liu, Y.; Dong, F.; Song, W.; Zhen, J.; Zhou, W.; Xu, H.; et al. Multiresistant ST59-SCCmec IV-t437 clone with strong biofilm-forming capacity was identified predominantly in MRSA isolated from Chinese children. *BMC Infect. Dis.* **2017**, *17*, 733.
- (7) Rolo, J.; Miragaia, M.; Turlej-Rogacka, A.; Empel, J.; Bouchami, O.; Faria, N. A.; Tavares, A.; Hryniewicz, W.; Fluit, A. C.; de Lencastre, H.; Group, C. W. High genetic diversity among community-associated *Staphylococcus aureus* in Europe: results from a multicenter study. *PLoS One* **2012**, *7*, No. e34768.
- (8) Glasner, C.; Pluister, G.; Westh, H.; Arends, J. P.; Empel, J.; Giles, E.; Laurent, F.; Layer, F.; Marstein, L.; Matussek, A.; et al. *Staphylococcus aureus* spa type t437: identification of the most dominant community-associated clone from Asia across Europe. *Clin. Microbiol. Infect.* **2015**, *21* (163), e161–e168.
- (9) Bonar, E.; Wojcik, I.; Wladyka, B. Proteomics in studies of *Staphylococcus aureus* virulence. *Acta Biochim Pol* **2015**, *62*, 367–381.
- (10) Dinges, M. M.; Orwin, P. M.; Schlievert, P. M. Exotoxins of *Staphylococcus aureus*. *Clin. Microbiol. Rev.* **2000**, *13*, 16–34.
- (11) Schlievert, P. M.; Strandberg, K. L.; Lin, Y.-C.; Peterson, M. L.; Leung, D. Y. M. Secreted virulence factor comparison between methicillin-resistant and methicillin-sensitive *Staphylococcus aureus*, and its relevance to atopic dermatitis. *J. Allergy Clin. Immunol.* **2010**, *125*, 39–49.
- (12) Wu, D.; Li, X.; Yang, Y.; Zheng, Y.; Wang, C.; Deng, L.; Liu, L.; Li, C.; Shang, Y.; Zhao, C.; et al. Superantigen gene profiles and presence of exfoliative toxin genes in community-acquired methicillin-resistant *Staphylococcus aureus* isolated from Chinese children. *J. Med. Microbiol.* **2011**, *60*, 35–45.
- (13) Busche, T.; Hillion, M.; Loi, V. V.; Berg, D.; Walther, B.; Semmler, T.; Strommenger, B.; Witte, W.; Cuny, C.; Mellmann, A.; et al. Comparative secretome analyses of human and zoonotic *Staphylococcus aureus* isolates of CC8, CC22 and CC398. *Mol. Cell. Proteomics* **2018**, *17*, 2412–2433.
- (14) Goldmann O, M. E *Staphylococcus aureus* strategies to evade the host acquired immune response. *Int. J. Med. Microbiol.* **2018**, *308*, 625–630.
- (15) Ziebandt, A. K.; Kusch, H.; Degner, M.; Jaglitz, S.; Sibbald, M. J.; Arends, J. P.; Chlebowicz, M. A.; Albrecht, D.; Pantucek, R.; Doskar, J.; et al. Proteomics uncovers extreme heterogeneity in the *Staphylococcus aureus* exoproteome due to genomic plasticity and variant gene regulation. *Proteomics* **2010**, *10*, 1634–1644.
- (16) Sibbald, M. J. B.; Ziebandt, A. K.; Engelmann, S.; Hecker, M.; de Jong, A.; Harmsen, H. J. M.; Raangs, G. C.; Stokroos, I.; Arends, J. P.; Dubois, J. Y. F.; van Dijk, J. M. Mapping the Pathways to Staphylococcal Pathogenesis by Comparative Secretomics. *Microbiol. Mol. Biol. Rev.* **2006**, *70*, 755–788.
- (17) Desbois, A. P.; Coote, P. J. Utility of Greater Wax Moth Larva (*Galleria mellonella*) for Evaluating the Toxicity and Efficacy of New Antimicrobial Agents. *Adv. Appl. Microbiol.* **2012**, *78*, 25–53.
- (18) Wojda, I. Immunity of the greater wax moth *Galleria mellonella*. *Insect Sci.* **2017**, *24*, 342–357.
- (19) Dreisbach, A.; Hempel, K.; Buist, G.; Hecker, M.; Becher, D.; van Dijk, J. M. Profiling the surfacome of *Staphylococcus aureus*. *Proteomics* **2010**, *10*, 3082–3096.
- (20) Koedijk, D.; Pastrana, F. R.; Hoekstra, H.; Berg, S. V. D.; Back, J. W.; Kerstholt, C.; Prins, R. C.; Bakker-Woudenberg, I.; van Dijk, J. M.; Buist, G. Differential epitope recognition in the immunodominant staphylococcal antigen A of *Staphylococcus aureus* by mouse versus human IgG antibodies. *Sci. Rep.* **2017**, *7*, 8141.
- (21) Aguilar, S. R.; Stulke, J.; van Dijk, J. M. Less is more: towards a genome-reduced *Bacillus* cell factory for 'difficult proteins'. *ACS Synth. Biol.* **2019**, *8*, 99.
- (22) Stobernack, T.; Glasner, C.; Junker, S.; Gabarrini, G.; de Smit, M.; de Jong, A.; Otto, A.; Becher, D.; van Winkelhoff, A. J.; van Dijk, J. M. Extracellular Proteome and Citrullinome of the Oral Pathogen *Porphyromonas gingivalis*. *J. Proteome Res.* **2016**, *15*, 4532–4543.
- (23) Koch, G.; Nadal-Jimenez, P.; Cool, R. H.; Quax, W. J. Assessing *Pseudomonas* virulence with nonmammalian host: *Galleria mellonella*. *Methods Mol. Biol.* **2014**, *1149*, 681–688.
- (24) Fey, P. D.; Endres, J. L.; Yajjala, V. K.; Widhelm, T. J.; Boissy, R. J.; Bose, J. L.; Bayles, K. W.; Bush, K. A Genetic Resource for Rapid and Comprehensive Phenotype Screening of Nonessential *Staphylococcus aureus* Genes. *mBio* **2013**, *4*, No. e00537–12.
- (25) Stapleton, M. R.; Horsburgh, M. J.; Hayhurst, E. J.; Wright, L.; Jonsson, I.-M.; Tarkowski, A.; Kokai-Kun, J. F.; Mond, J. J.; Foster, S. J. Characterization of IsaA and ScaD, Two Putative Lytic Transglycosylases of *Staphylococcus aureus*. *J. Bacteriol.* **2007**, *189*, 7316–7325.
- (26) Krogh, A.; Larsson, B.; von Heijne, G.; Sonnhammer, E. L. L. Predicting transmembrane protein topology with a hidden markov model: application to complete genomes. Edited by F. Cohen. *J. Mol. Biol.* **2001**, *305*, 567–580.
- (27) Petersen, T. N.; Brunak, S.; von Heijne, G.; Nielsen, H. SignalP 4.0: discriminating signal peptides from transmembrane regions. *Nat. Methods* **2011**, *8*, 785–786.
- (28) Berven, F. S.; Karlsen, O. A.; Straume, A. H.; Flikka, K.; Murrell, J. C.; Fjellbirkeland, A.; Lillehaug, J. R.; Eidhammer, I.; Jensen, H. B. Analysing the outer membrane subproteome of *Methylococcus capsulatus* (Bath) using proteomics and novel biocomputing tools. *Arch. Microbiol.* **2006**, *184*, 362–377.
- (29) Yu, N. Y.; Wagner, J. R.; Laird, M. R.; Melli, G.; Rey, S.; Lo, R.; Dao, P.; Sahinalp, S. C.; Ester, M.; Foster, L. J.; Brinkman, F. S. L. PSORTb 3.0: improved protein subcellular localization prediction with refined localization subcategories and predictive capabilities for all prokaryotes. *Bioinformatics* **2010**, *26*, 1608–1615.
- (30) Clark, H. F. The Secreted Protein Discovery Initiative (SPDI), a Large-Scale Effort to Identify Novel Human Secreted and Transmembrane Proteins: A Bioinformatics Assessment. *Genome Res.* **2003**, *13*, 2265–2270.
- (31) Bendtsen, J. D.; Kiemer, L.; Fausboll, A.; Brunak, S. Non-classical protein secretion in bacteria. *BMC Microbiol.* **2005**, *5*, 58.
- (32) Liebermeister, W.; Noor, E.; Flamholz, A.; Davidi, D.; Bernhardt, J.; Milo, R. Visual account of protein investment in cellular functions. *Proc. Natl. Acad. Sci. U. S. A.* **2014**, *111*, 8488–8493.
- (33) Team TRDC. R: A Language and Environment for Statistical Computing; R Foundation for Statistical Computing: Vienna, Austria, 2013; <http://www.R-project.org/>.
- (34) Mundt AKaF. *factoextra: Extract and Visualize the Results of Multivariate Data Analyses*; 2017; <https://CRAN.R-project.org/package=factoextra>.
- (35) Mader, U.; Nicolas, P.; Depke, M.; Pane-Farre, J.; Debarbouille, M.; van der Kooij-Pol, M. M.; Guerin, C.; Derozier, S.; Hiron, A.; Jarmer, H.; et al. *Staphylococcus aureus* Transcriptome Architecture: From Laboratory to Infection-Mimicking Conditions. *PLoS Genet.* **2016**, *12*, No. e1005962.
- (36) Lowy, M. D. *Staphylococcus aureus* infection. *N. Engl. J. Med.* **1998**, *339*, 520–532.

- (37) Lorenz, U.; Ohlsen, K.; Karch, H.; Hecker, M.; Thiede, A.; Hacker, J. Human antibody response during sepsis against targets expressed by methicillin resistant *Staphylococcus aureus*. *FEMS Immunol. Med. Microbiol.* **2000**, *29*, 145–153.
- (38) van den Berg, S.; Bonarius, H. P. J.; van Kessel, K. P. M.; Elsinga, G. S.; Kooi, N.; Westra, H.; Bosma, T.; van der Kooi-Pol, M. M.; Koedijk, D. G. A. M.; Groen, H.; et al. A human monoclonal antibody targeting the conserved staphylococcal antigen IsaA protects mice against *Staphylococcus aureus* bacteremia. *Int. J. Med. Microbiol.* **2015**, *305*, 55–64.
- (39) Krishnappa, L.; Dreisbach, A.; Otto, A.; Goosens, V. J.; Cranenburgh, R. M.; Harwood, C. R.; Becher, D.; van Dijk, J. M. Extracytoplasmic proteases determining the cleavage and release of secreted proteins, lipoproteins, and membrane proteins in *Bacillus subtilis*. *J. Proteome Res.* **2013**, *12*, 4101–4110.
- (40) Guinane, C. M.; Penades, J. R.; Fitzgerald, J. R. The role of horizontal gene transfer in *Staphylococcus aureus* host adaptation. *Virulence* **2011**, *2*, 241–243.
- (41) Mekonnen, S. A.; Palma Medina, L. M.; Glasner, C.; Tsompanidou, E.; de Jong, A.; Grasso, S.; Schaffer, M.; Mader, U.; Larsen, A. R.; Gumpert, H.; et al. Signatures of cytoplasmic proteins in the exoproteome distinguish community- and hospital-associated methicillin-resistant *Staphylococcus aureus* USA300 lineages. *Virulence* **2017**, *8*, 891–907.
- (42) Liew, Y. K.; Hamat, R. A.; Nordin, S. A.; Chong, P. P.; Neela, V. The exoproteomes of clonally related *Staphylococcus aureus* strains are diverse. *Ann. Microbiol.* **2015**, *65*, 1809–1813.
- (43) Ebner, P.; Prax, M.; Nega, M.; Koch, I.; Dube, L.; Yu, W.; Rinker, J.; Popella, P.; Flotenmeyer, M.; Gotz, F. Excretion of cytoplasmic proteins (ECP) in *Staphylococcus aureus*. *Mol. Microbiol.* **2015**, *97*, 775–789.
- (44) Gotz, F.; Yu, W.; Dube, L.; Prax, M.; Ebner, P. Excretion of cytosolic proteins (ECP) in bacteria. *Int. J. Med. Microbiol.* **2015**, *305*, 230–237.
- (45) Byrum, S. D.; Loughran, A. J.; Beenken, K. E.; Orr, L. M.; Storey, A. J.; Mackintosh, S. G.; Edmondson, R. D.; Tackett, A. J.; Smeltzer, M. S. Label-Free Proteomic Approach to Characterize Protease-Dependent and -Independent Effects of sarA Inactivation on the *Staphylococcus aureus* Exoproteome. *J. Proteome Res.* **2018**, *17*, 3384–3395.
- (46) Ebner, P.; Rinker, J.; Gotz, F. Excretion of cytoplasmic proteins in *Staphylococcus* is most likely not due to cell lysis. *Curr. Genet.* **2016**, *62*, 19–23.
- (47) Ebner, P.; Luqman, A.; Reichert, S.; Hauf, K.; Popella, P.; Forchhammer, K.; Otto, M.; Gotz, F. Non-classical Protein Excretion Is Boosted by PSMalpha-Induced Cell Leakage. *Cell Rep.* **2017**, *20*, 1278–1286.
- (48) Schlag, M.; Biswas, R.; Krismer, B.; Kohler, T.; Zoll, S.; Yu, W.; Schwarz, H.; Peschel, A.; Gotz, F. Role of staphylococcal wall teichoic acid in targeting the major autolysin Atl. *Mol. Microbiol.* **2010**, *75*, 864–873.
- (49) Gotz, F.; Hacker, J.; Hecker, M. Pathophysiology of staphylococci in the post-genomic era. *Int. J. Med. Microbiol.* **2010**, *300*, 75.
- (50) Krishnappa, L.; Dreisbach, A.; Otto, A.; Goosens, V. J.; Cranenburgh, R. M.; Harwood, C. R.; Becher, D.; van Dijk, J. M. Extracytoplasmic proteases determining the cleavage and release of secreted proteins, lipoproteins, and membrane proteins in *Bacillus subtilis*. *J. Proteome Res.* **2013**, *12*, 4101–4110.
- (51) van Wamel, W. J.; Rooijackers, S. H.; Ruyken, M.; van Kessel, K. P.; van Strijp, J. A. The innate immune modulators staphylococcal complement inhibitor and chemotaxis inhibitory protein of *Staphylococcus aureus* are located on beta-hemolysin-converting bacteriophages. *J. Bacteriol.* **2006**, *188*, 1310–1315.
- (52) Antelmann, H.; Tjalsma, H.; Voigt, B.; Ohlmeier, S.; Bron, S.; van Dijk, J. M.; Hecker, M. A proteomic view on genome-based signal peptide predictions. *Genome Res.* **2001**, *11*, 1484–1502.
- (53) Kolar, S. L.; Ibarra, J. A.; Rivera, F. E.; Mootz, J. M.; Davenport, J. E.; Stevens, S. M.; Horswill, A. R.; Shaw, L. N. Extracellular proteases are key mediators of *Staphylococcus aureus* virulence via the global modulation of virulence-determinant stability. *MicrobiologyOpen* **2013**, *2*, 18–34.
- (54) Kainulainen, V.; Korhonen, T. K. Dancing to another tune—adhesive moonlighting proteins in bacteria. *Biology (Basel, Switz.)* **2014**, *3*, 178–204.
- (55) Jin, H.; Song, Y. P.; Boel, G.; Kochar, J.; Pancholi, V. Group A streptococcal surface GAPDH, SDH, recognizes uPAR/CD87 as its receptor on the human pharyngeal cell and mediates bacterial adherence to host cells. *J. Mol. Biol.* **2005**, *350*, 27–41.
- (56) Crowe, J. D.; Sievwright, I. K.; Auld, G. C.; Moore, N. R.; Gow, N. A.; Booth, N. A. *Candida albicans* binds human plasminogen: identification of eight plasminogen-binding proteins. *Mol. Microbiol.* **2003**, *47*, 1637–1651.
- (57) Tunio, S. A.; Oldfield, N. J.; Berry, A.; Ala'Aldeen, D. A.; Wooldridge, K. G.; Turner, D. P. The moonlighting protein fructose-1, 6-bisphosphate aldolase of *Neisseria meningitidis*: surface localization and role in host cell adhesion. *Mol. Microbiol.* **2010**, *76*, 605–615.
- (58) Lechardeur, D.; Fernandez, A.; Robert, B.; Gaudu, P.; Trieu-Cuot, P.; Lamberet, G.; Gruss, A. The 2-Cys peroxiredoxin alkyl hydroperoxide reductase c binds heme and participates in its intracellular availability in *Streptococcus agalactiae*. *J. Biol. Chem.* **2010**, *285*, 16032–16041.
- (59) N'Diaye, A.; Mijouin, L.; Hillion, M.; Diaz, S.; Konto-Ghiorghi, Y.; Percoco, G.; Chevalier, S.; Lefevre, L.; Harmer, N. J.; Lesouhaitier, O.; Feuilloley, M. G. J. Effect of Substance P in *Staphylococcus aureus* and *Staphylococcus epidermidis* Virulence: Implication for Skin Homeostasis. *Front. Microbiol.* **2016**, *7*, 506.
- (60) Dallo, S. F.; Kannan, T. R.; Blaylock, M. W.; Baseman, J. B. Elongation factor Tu and E1 beta subunit of pyruvate dehydrogenase complex act as fibronectin binding proteins in *Mycoplasma pneumoniae*. *Mol. Microbiol.* **2002**, *46*, 1041–1051.
- (61) Fedhila, S.; Buisson, C.; Dussurget, O.; Serror, P.; Glomski, I. J.; Liehl, P.; Lereclus, D.; Nielsen-LeRoux, C. Comparative analysis of the virulence of invertebrate and mammalian pathogenic bacteria in the oral insect infection model *Galleria mellonella*. *J. Invertebr. Pathol.* **2010**, *103*, 24–29.
- (62) Brennan, M.; Thomas, D. Y.; Whiteway, M.; Kavanagh, K. Correlation between virulence of *Candida albicans* mutants in mice and *Galleria mellonella* larvae. *FEMS Immunol. Med. Microbiol.* **2002**, *34*, 153–157.
- (63) Ziebandt, A.-K.; Becher, D.; Ohlsen, K.; Hacker, J.; Hecker, M.; Engelmann, S. The influence of agr and σ B in growth phase dependent regulation of virulence factors in *Staphylococcus aureus*. *Proteomics* **2004**, *4*, 3034–3047.
- (64) Peleg, A. Y.; Monga, D.; Pillai, S.; Mylonakis, E.; Moellering, R. C., Jr.; Eliopoulos, G. M. Reduced susceptibility to vancomycin influences pathogenicity in *Staphylococcus aureus* infection. *J. Infect. Dis.* **2009**, *199*, 532–536.
- (65) Lorenz, U.; Lorenz, B.; Schmitter, T.; Streker, K.; Erck, C.; Wehland, J.; Nickel, J.; Zimmermann, B.; Ohlsen, K. Functional antibodies targeting IsaA of *Staphylococcus aureus* augment host immune response and open new perspectives for antibacterial therapy. *Antimicrob. Agents Chemother.* **2011**, *55*, 165–173.
- (66) Romero Pastrana, F.; Thompson, J. M.; Heuker, M.; Hoekstra, H.; Dillen, C. A.; Ortines, R. V.; Ashbaugh, A. G.; Pickett, J. E.; Linssen, M. D.; Bernthal, N. M.; et al. Noninvasive optical and nuclear imaging of *Staphylococcus*-specific infection with a human monoclonal antibody-based probe. *Virulence* **2018**, *9*, 262–272.
- (67) Rathore, A. S.; Gupta, R. D. Chitinases from Bacteria to Human: Properties, Applications, and Future Perspectives. *Enzyme Res.* **2015**, *2015*, 791907.
- (68) Da Silva, C. A.; Chalouni, C.; Williams, A.; Hartl, D.; Lee, C. G.; Elias, J. A. Chitin is a size-dependent regulator of macrophage TNF and IL-10 production. *J. Immunol.* **2009**, *182*, 3573–3582.